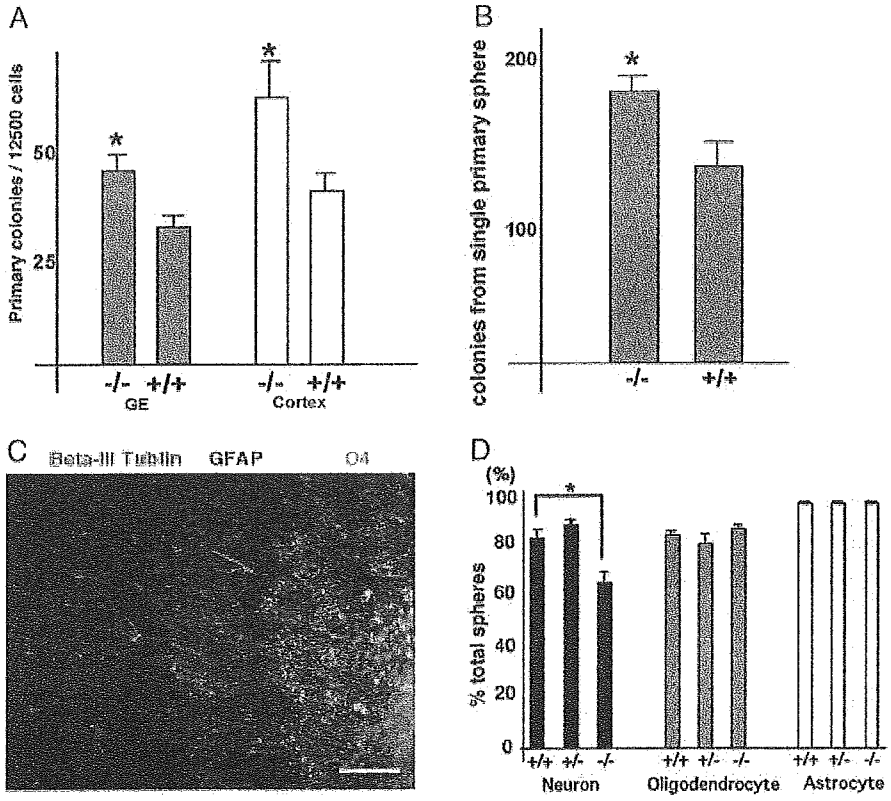

Fig. 3. Examination of neurosphere formation and differentiation in *HuD*-deficient embryos. (*A*) The number of neurospheres generated from 12,500 cells derived from the ganglionic eminence (GE) and cerebral cortex (Cortex) of E14.5 embryos, in 500 μl of the proliferation medium. (*B*) The number of secondary spheres derived from a single dissociated primary neurosphere is shown. (*C*) After allowing 72 h of differentiation of the primary neurospheres, the cell sheets generated from the neurospheres were fixed and triple-immunostained by using anti-TuJ1 (red), GFAP (blue), and O4 (green) antibodies. (Bar, 300 μm.) (*D*) The differentiation capacity of each primary neurosphere was determined based on the cell types contained in each clone. The clone types were analyzed for 100 spheres from each genotype.

HuD−/− mice than in their wild-type littermates. The number of primary spheres forming cells was also increased in the *HuD*−/− embryonic cerebral cortex. The number of secondary neurospheres generated from the subcloning of a single primary neurosphere may be considered as an estimate of the extent to which the initial primary neurosphere-forming stem cell undergoes symmetric divisions (18). The number of secondary neurosphere colonies was also significantly increased in E14.5 *HuD*−/− brains as compared with that in the brains of their wild-type controls (Fig. 3*B*), suggesting that the sphere-forming cells derived from E14.5 *HuD*−/− brains exhibited enhanced self-renewal capacity.

Next, we tested the multipotency of the neural stem cells by the differentiation assay; each neurosphere can be induced to differentiate into TuJ1-expressing neurons (N), GFAP-expressing astrocytes (A), and/or O4-expressing oligodendrocytes (O). After allowing differentiation to take place for 72 h, the cell sheets generated from the neurospheres were fixed and triple-immunostained by using anti-TuJ1, anti-GFAP, and anti-O4 antibody (Fig. 3*C*). Then, each sphere was analyzed for NAO expression. The number of spheres that generated neurons was significantly decreased to 0.8-fold in the *HuD*−/− embryos (Fig. 3*D*), whereas the number of spheres that generated oligodendrocytes and astrocytes remained unchanged (Fig. 3*D*). These observations indicate that the neural stem cells in E14.5 *HuD*−/− embryos have increased self-renewal ability and reduced ability to differentiate into neuronal progeny.

To investigate the *in vivo* kinetics of neurogenesis (production of postmitotic neurons) in the *HuD*-deficient embryonic cerebral wall, we performed sequential labeling for S phase markers by using IdUrd and BrdUrd, as described in previous reports, except that IdUrd was used in the place of tritiated thymidine (19). Using BrdUrd-only cumulative labeling, we could not observe any visible differences in the cell cycle length of the proliferative cells in the embryonic pseudostratified ventricular epithelium (PVE) between *HuD*−/− and wild-type mice (data not shown). Therefore, we concluded that 14.5 h of continuous BrdUrd exposure as described (22) was sufficiently long to cover the duration of the total cell cycle length (Tc); the S-phase length was then subtracted from Tc to calculate the percentage of mitotically Q cells, which represents the percentage of postmitotic neurons in this region. The distribution of Q cells and P + Q cells in the *HuD*−/− and wild-type embryos is shown in Fig. 4 *A* and *B*. In the case of the wild-type mice, the Q cells were mainly localized at a distance of 80–100 μm from the lateral ventricular surface, which corresponds to the position at which the cells leave the cell cycle and migrate out from the PVE (19). In the *HuD*−/− embryos, the number of Q cells (Fig. 4*B*) in these regions was decreased as compared with that in the wild-type embryos. In contrast, the number of P + Q cells (Fig. 4*A*) was not changed. Total numbers of P and P + Q cells in intermediate zone (bin6–16) are shown in Fig. 4*C*. The ratio of Q cells is calculated as N(Q)/N(P + Q). This value (Q fraction) represents the ratio of cells exit from cell cycles during G_1 phase. A decreased Q fraction in *HuD*−/− embryos suggests that the number and ratio of cells leaving the cell cycle are decreased, and that the P population in the developing cerebral wall is increased in the *HuD*−/− embryos and further suggests that in the absence of *HuD*, some of the neural stem/progenitor cells or committed neuronal progenitor cells fail to leave the cell cycle, resulting in reduced production of postmitotic neurons.

Macrocephaly has been described in several mutant mice lacking negative regulators of the cell cycle: Mice deficient in PTEN, a negative regulator of the cell cycle in neural stem cells (23), as well as those deficient in the cyclin-dependent kinase inhibitor p27(Kip1), a putative target of the Hu proteins (6, 24), show the macrocephaly phenotype in common, and these phenotypes are compatible with that predicted by theoretical simulation in the mathematical model of neocortical histogenesis (22). However, we found that the actual size of the postnatal brain was not larger in the

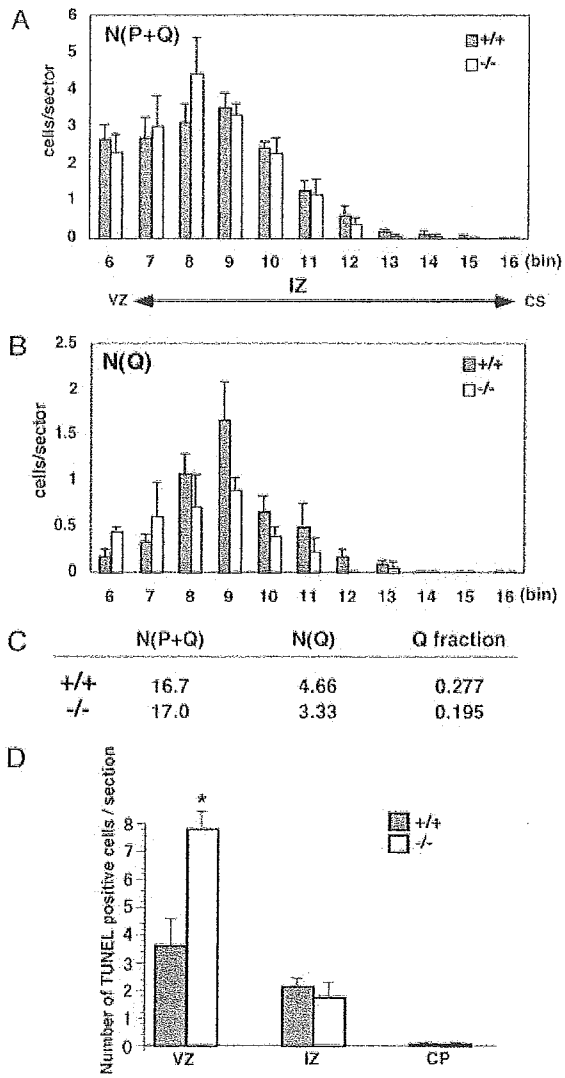

Fig. 4. Cohort analysis of cellular proliferation in the embryonic cerebral wall. (*A* and *B*) The distributions of the cells in the P + Q (*A*) or Q (*B*) fractions of the E14 *HuD*−/− and wild-type embryos. The analysis was undertaken in a coronal sector of the dorsomedial cerebral wall, ≈100 μm thick in its medial–lateral dimension and 4 μm thick (corresponding to the section thickness) in its rostral–caudal dimension. The sector was divided in its radial dimension into bins (*x* axis) 10 μm in height and numbered 1, 2, 3, and so on, from the ventricular margin. The numbers of cells in the Q or P + Q fraction [N(Q) or N(P+Q)] for each bin (*y* axis) were determined by counting only cells labeled by IdUrd in each protocol. IZ, intermediate zone; VZ, ventricular zone; and CS, cortical surface. (*C*) Total number of N(P + Q) and N(Q) cells in 5–16 bins is shown. Q fraction is calculated as N(Q)/N(P + Q). (*D*) Apoptotic cells in 4-μm-thick paraffin-embedded coronal sections of *HuD*−/− and wild-type embryos were detected by using the TUNEL method. The number of TUNEL-positive cells present along the lateral ventricular wall in the medial cerebral wall was counted. The apoptotic cells were then classified according to their location, based on the histological structure of the sections (IZ, intermediate zone; and CP, cortical plate).

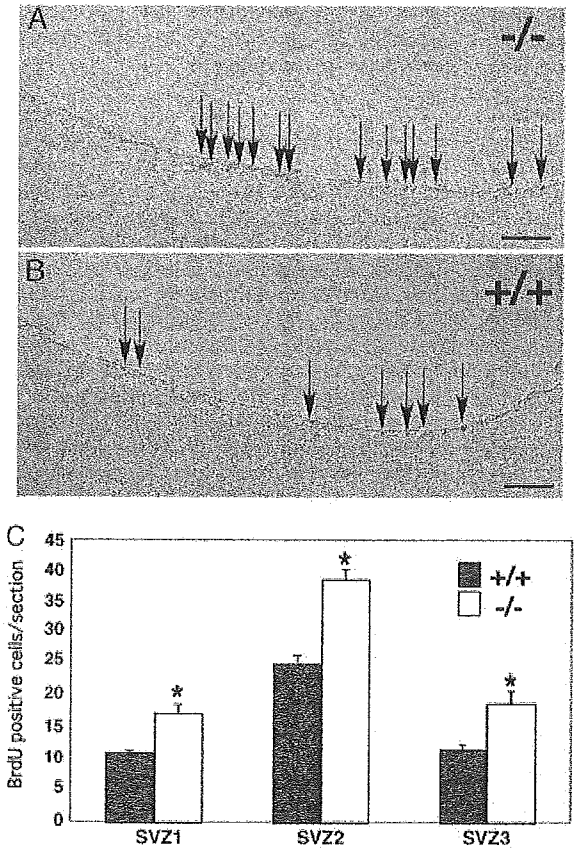

Fig. 5. Slowly dividing cells in the SVZ of adult *HuD*-deficient mice. (*A* and *B*) BrdUrd-labeled cells in the SVZ of *HuD*−/− mice (*B*) and their wild-type littermates were detected by immunostaining by using anti-BrdUrd monoclonal antibody. BrdUrd-positive cells are indicated by arrows. (Bar, 100 μm.) (*C*) The number of BrdUrd- positive cells in each of the frontal levels of the lateral SVZ in the animals was calculated. Three different frontal levels were analyzed. From rostral to caudal, slices were classified in three levels, SVZ1, SVZ2, and SVZ3 (also see Fig. 8).

HuD−/− mice. This discrepancy may be accounted for by increased apoptosis within the progenitor population. To investigate this possibility, we evaluated the status of apoptosis in the *HuD*−/− embryonic cerebral cortex (Fig. 4*D*). The number of apoptotic cells, as detected by the TUNEL method, was 2.2-fold higher in the ventricular zone, but not in the intermediate zone and cortical plate, of the *HuD*−/− as compared with that in their wild-type littermates. These data suggest that at least some of the cells that fail to leave the cell cycle undergo apoptosis, possibly due to their inability to undergo appropriate neuronal differentiation.

The Number of Slowly Dividing Stem Cells Is Increased in the SVZ of Adult *HuD*-Deficient Mice. It has been reported that several neurogenic regions are present in the adult mouse brain. Slowly dividing cells present in the adult SVZ are believed to exhibit neural stem-cell activities (25). To label slowly proliferating cells *in vivo*, adult *HuD*−/− and WT mice were administered BrdUrd continuously for 4 weeks, followed by a BrdUrd-free chase period of 1 week. For quantification of the labeled cells, we subdivided the lateral ventricle into three distinct coronal levels (Fig. 8, which is published as supporting information on the PNAS web site). Cells labeled with BrdUrd were visualized by immunohistochemical staining by using anti-BrdUrd antibody (Fig. 5 *A* and *B*). BrdUrd-positive cells were present within the SVZ along the lateral ventricular wall. At all of the coronal levels analyzed (SVZ1, -2, and -3), the total number of BrdUrd-positive cells was 1.5- to 2.0-fold higher in the *HuD*−/− mice than in their wild-type littermates (Fig. 5*C*).

These results taken together suggest that the neural stem/progenitor cells in both fetal (embryonic periventricular and embryonic ganglionic eminence cells; Figs. 3 and 4) and adult (SVZ cells in the adult; Fig. 5) brains exhibit increased self-renewal

activity in *HuD*−/− mice. Disruption of the *HuD* gene had similar positive effects on the cellular P behavior of the neural progenitor/stem cells derived from these three regions.

Discussion

Interestingly, we found that the ratio of neuron-producing neurospheres is decreased in *HuD*−/− mice. This could be interpreted as suggesting that HuD is required for (*i*) neuronal commitment of neural stem/progenitor cells, (*ii*) selective survival of neuronally committed progenitor cells, and/or (*iii*) production of postmitotic neurons from neuronal progenitor cells. The increased self-renewal activity of neural stem/progenitor cells observed in *HuD*−/− mice (Fig. 3) might lend the strongest support to the first possibility above. However, this issue should be investigated further in depth, because the latter two indicate the possible roles of HuD in committed neuronal progenitor cells. A previous study characterizing the expression of Hu proteins in subependymal zone cells of the adult songbird forebrain indicates that Hu proteins begin to be expressed in the neuronally committed progenitor cells only after the S phase, during either the premitotic G_2 phase of the progenitor cells or the early G_0/G_1 phase of the daughter cells (26). Furthermore, it was reported that *HuD* mRNA was expressed mainly in the intermediate and outer ventricular zones of the cortex, rather than in the cortical plate in E14.5 mice (4). In the spinal cord of stage 17 chick embryos, *HuD* mRNA was shown to be mainly localized in the ventral immature neuronal progeny, where the immunoreactivity of the 16A11(HuB/HuC/HuD) monoclonal antibody has not yet been seen (27). Taken together, it might be feasible to suggest that HuD commences its expression in proliferative neuronal progenitor cells and drives them to exit the mitotic cycle. We also found that the percentage of spheres that generate oligodendrocytes and astrocytes was not significantly changed in *HuD*−/− mice, indicating that HuD may not be involved in glial cell fate determination, and that its roles may be restricted to only the neuronally committed lineage.

The transcripts of p27 and p21, both cyclin-dependent kinase (CDK) inhibitors, have been reported as the binding targets of the Hu proteins. They are known to be involved in the acquisition of postmitotic phenotypes in the cells of neuronal lineages. Although overexpression of the Hu proteins in SH-SY5Y or PC12 cells induced the expression of CDK inhibitor proteins and growth arrest (W.A. and H.O., unpublished results), we could not detect any differences in the expression patterns or expression levels of the CDK inhibitors between *HuD*−/− mice and their wild-type littermates. It should be further investigated whether they are regulated by the Hu proteins and induce cell cycle exit of neuronal progenitors *in vivo*. Although HuD seems to be down-regulated in postmitotic mature neurons, it might still be required for the acquisition of the fully differentiated characteristics and various functions of mature neurons, including neurite extension and expression of neuronal markers. The mRNA of several neuronal proteins, including tau, GAP-43, and Neuroserpin, which are involved in the structure (e.g., neurite extension) and function of neurons, has also been reported to bind between their mRNA and Hu proteins (9, 10, 28). In this *HuD*−/− model, we examined the expression of GAP-43 and p27 protein by immunoblotting (Fig. 9, which is published as supporting information on the PNAS web site). We also examined the expression of tau mRNA by using real-time quantitive PCR in E17 brain (data not shown). Although we could not detect any significant difference in the expression of these molecules between *HuD*+/+ and *HuD*−/− mice, our observations do not directly deny the previous results of the study on GAP-43, p27, and tau. Even if not up-regulated, other Hu protein might have compensated the loss of *HuD* because of the functional redundancy of Hu-family proteins. Impaired cranial nerve development phenotype in E10.5 embryos (Fig. 2 *A–D*), impaired rotarod performance (Fig. 2*G*), and abnormal clasping reflex in the *HuD*−/− mice might lend support to such possibilities.

Conclusion

Based on the present loss-of-function studies, we suggest that HuD may be involved at multiple stages during neuronal development: (*i*) HuD negatively regulates the proliferation of neural stem/progenitor cells, (*ii*) HuD promotes the exit of neuronally committed progenitor cells from the cell cycle, and (*iii*) HuD promotes the differentiation of postmitotic neurons. It is of note that although the time of onset of the expression is, to some extent at least, specific for each of the HuB/C/D proteins (4), members of the Hu-family proteins showed marked similarities in their primary structures, expression profiles, and functions, as revealed by their misexpression studies. Thus, partially redundant functions of the different Hu proteins might mask the actual phenotype of the *HuD*-deficient mice in a developmental-stage-dependent manner (Fig. 2). Because our *HuD*-deficient mice were generated by an irremovable PGK-neocassette, and we cannot completely exclude the altered expression of neighborhood genes (29), future studies of multiple and conditional targeted disruptions using Cre-loxP system with a reversible neocassette may reveal the *in vivo* functions of Hu proteins in greater detail.

We thank Dr. Shin-ichiro Imai for technical assistance and helpful comments and Drs. Noriko Osumi, Takuya Shimazaki, and Kazunobu Sawamoto and members of the Okano laboratory for valuable discussions. This work was supported by grants from the Japanese Ministry of Education, Sports and Culture of Japan (to H.O.) and by a grant from the 21st Century Centers of Excellence Program of the Ministry of Education, Science and Culture of Japan (to Keio University).

1. Szabo, A., Dalmau, J., Manley, G., Rosenfeld, M., Wong, E., Henson, J., Posner, J. B. & Furneaux, H. M. (1991) *Cell* **67,** 325–333.
2. Ma, W. J., Cheng, S., Campbell, C., Wright, A. & Furneaux, H. (1996) *J. Biol. Chem.* **271,** 8144–8151.
3. Levine, T. D., Gao, F., King, P. H., Andrews, L. G. & Keene, J. D. (1993) *Mol. Cell. Biol.* **13,** 3494–3504.
4. Okano, H. J. & Darnell, R. B. (1997) *J. Neurosci.* **17,** 3024–3037.
5. Joseph, B., Orlian, M. & Furneaux, H. (1998) *J. Biol. Chem.* **273,** 20511–20516.
6. Kullmann, M., Gopfert, U., Siewe, B. & Hengst, L. (2002) *Genes Dev.* **16,** 3087–3099.
7. Ross, R. A., Lazarova, D. L., Manley, G. T., Smitt, P. S., Spengler, B. A., Posner, J. B. & Biedler, J. L. (1997) *Eur. J. Cancer* **33,** 2071–2074.
8. Antic, D., Lu, N. & Keene, J. D. (1999) *Genes Dev.* **13,** 449–461.
9. Chung, S., Eckrich, M., Perrone-Bizzozero, N., Kohn, D. T. & Furneaux, H. (1997) *J. Biol. Chem.* **272,** 6593–6598.
10. Aranda-Abreu, G. E., Behar, L., Chung, S., Furneaux, H. & Ginzburg, I. (1999) *J. Neurosci.* **19,** 6907–6917.
11. Atlas, R., Behar, L., Elliott, E. & Ginzburg, I. (2004) *J. Neurochem.* **89,** 613–626.
12. Akamatsu, W., Okano, H. J., Osumi, N., Inoue, T., Nakamura, S., Sakakibara, S., Miura, M., Matsuo, N., Darnell, R. B. & Okano, H. (1999) *Proc. Natl. Acad. Sci. USA* **96,** 9885–9890.
13. Kasashima, K., Terashima, K., Yamamoto, K., Sakashita, E. & Sakamoto, H. (1999) *Genes Cells* **4,** 667–683.
14. Quattrone, A., Pascale, A., Nogues, X., Zhao, W., Gusev, P., Pacini, A. & Alkon, D. L. (2001) *Proc. Natl. Acad. Sci. USA* **98,** 11668–11673.
15. Sakakibara, S., Nakamura, Y., Yoshida, T., Shibata, S., Koike, M., Takano, H., Ueda, S., Uchiyama, Y., Noda, T. & Okano, H. (2002) *Proc. Natl. Acad. Sci. USA* **99,** 15194–15199.
16. Osumi, N., Hirota, A., Ohuchi, H., Nakafuku, M., Iimura, T., Kuratani, S., Fujiwara, M., Noji, S. & Eto, K. (1997) *Development (Cambridge, U.K.)* **124,** 2961–2972.
17. Hitoshi, S., Alexson, T., Tropepe, V., Donoviel, D., Elia, A. J., Nye, J. S., Conlon, R. A., Mak, T. W., Bernstein, A. & van der Kooy, D. (2002) *Genes Dev.* **16,** 846–858.
18. Reynolds, B. A. & Weiss, S. (1992) *Science* **255,** 1707–1710.
19. Takahashi, T., Nowakowski, R. S. & Caviness, V. S., Jr. (1996) *J. Neurosci.* **16,** 6183–6196.
20. Baquet, Z. C., Gorski, J. A. & Jones, K. R. (2004) *J. Neurosci.* **24,** 4250–4258.
21. Mangiarini, L., Sathasivam, K., Seller, M., Cozens, B., Harper, A., Hetherington, C., Lawton, M., Trottier, Y., Lehrach, H., Davies, S. W., *et al.* (1996) *Cell* **87,** 493–506.
22. Takahashi, T., Nowakowski, R. S. & Caviness, V. S., Jr. (1997) *Dev. Neurosci.* **19,** 17–22.
23. Groszer, M., Erickson, R., Scripture-Adams, D. D., Lesche, R., Trumpp, A., Zack, J. A., Kornblum, H. I., Liu, X. & Wu, H. (2001) *Science* **294,** 2186–2189.
24. Nakayama, K., Ishida, N., Shirane, M., Inomata, A., Inoue, T., Shishido, N., Horii, I. & Loh, D. Y. (1996) *Cell* **85,** 707–720.
25. Morshead, C. M., Reynolds, B. A., Craig, C. G., McBurney, M. W., Staines, W. A., Morassutti, D., Weiss, S. & van der Kooy, D. (1994) *Neuron* **13,** 1071–1082.
26. Barami, K., Iversen, K., Furneaux, H. & Goldman, S. A. (1995) *J. Neurobiol.* **28,** 82–101.
27. Wakamatsu, Y. & Weston, J. A. (1997) *Development (Cambridge, U.K.)* **124,** 3449–3460.
28. Cuadrado, A., Garcia-Fernandez, L. F., Imai, T., Okano, H. & Munoz, A. (2002) *Mol. Cell Neurosci.* **20,** 198–210.
29. Olson, E. N., Arnold, H. H., Rigby, P. W. & Wold, B. J. (1996) *Cell* **85,** 1–4.

Available online at www.sciencedirect.com
SCIENCE DIRECT
Experimental Cell Research 306 (2005) 349–356
Experimental Cell Research
www.elsevier.com/locate/yexcr

Review

Function of RNA-binding protein Musashi-1 in stem cells☆

Hideyuki Okano*, Hironori Kawahara, Masako Toriya, Keio Nakao, Shinsuke Shibata, Takao Imai

Department of Physiology, Keio University School of Medicine, 35 Shinanomachi, Shinjuku-ku, Tokyo 160-8582, Japan

Received 26 January 2005, revised version received 21 February 2005
Available online 24 March 2005

Abstract

Musashi is an evolutionarily conserved family of RNA-binding proteins that is preferentially expressed in the nervous system. The first member of the Musashi family was identified in *Drosophila*. This protein plays an essential role in regulating the asymmetric cell division of ectodermal precursor cells known as sensory organ precursor cells through the translational regulation of target mRNA. In the CNS of *Drosophila* larvae, however, Musashi is expressed in proliferating neuroblasts and likely has a different function. Its probable mammalian homologue, Musashi-1, is a neural RNA-binding protein that is strongly expressed in fetal and adult neural stem cells (NSCs). Mammalian Musashi-1 augments Notch signaling through the translational repression of its target mRNA, m-Numb, thereby contributing to the self-renewal of NSCs. In addition to its functions in NSCs, the role of mammalian Musashi-1 protein in epithelial stem cells, including intestinal and mammary gland stem cells, is attracting increasing interest.

Keywords: Musashi; Translational regulation; Neural stem cell; Intestinal stem cell; Mammary gland stem cell; Notch signaling; Numb

Contents

Introduction

Neural stem cells (NSCs) are deserving of attention in terms of strategies for central nervous system (CNS) regeneration, but what kind of cells are they? NSCs are the organ (tissue) stem cells that reside in the organs (tissues) that are referred to as the CNS. Tissue stem cells are undifferentiated cells found in many adult tissues and possess certain fundamental properties in common, including multipotency (the ability to differentiate into the various cells that compose tissues), ability to self-renew, and ability to repair damaged tissue. The evidence regarding tissue stem cells obtained thus far suggests that in besides being present in the hematopoietic system, stem cells or stem-cell-like cells are present in the liver, intestine, mammary gland, testis, skeletal muscle, skin, hair follicles, myocardium, and neural crest-derived tissue, as well as in the CNS [1]. It is

☆ Invited minireview on a special issue "Molecular control of cellular differentiation".

* Corresponding author. Fax: +81 3 3357 5445.
E-mail address: hidokano@sc.itc.keio.ac.jp (H. Okano).

0014-4827/$ - see front matter © 2005 Elsevier Inc. All rights reserved.
doi:10.1016/j.yexcr.2005.02.021

surprising and very interesting that tissue stem cells are not only present in the hematopoietic system, intestine, and skin, which have rapid physiological cell turnover rates, but also in organs with slow physiological cell turnover rates that would be expected to have extremely poor ability to regenerate, including CNS.

NSCs are the tissue stem cells that are present in the CNS, and they can be defined conceptually as cells that possess a combination of multipotency and ability to self-renew. Great strides have been made in research on NSCs during approximately the past 10 years, and the main driving force behind this progress seems to have been the development of (i) a group of selective marker molecules for neural stem/progenitor cells, (ii) selective culture methods for NSCs, and (iii) methods for prospective identification and isolation of NSCs. We will leave detailed overall explanations of each of them to review articles [2–4] and the corresponding original articles, but our research group takes pride in the fact that we have made major contributions to the development of neural stem cell research tools. Although it is impossible to strictly discriminate between NSCs and progenitor cells based on whether they express a group of selective neural stem/progenitor cell marker molecules, a great deal of circumstantial evidence has indicated that the level of expression of the RNA-binding protein Musashi-1 [5–7], the intermediate filament Nestin [8,9], and the transcription factor Sox (*S*RY-like HMG b*ox*)-family molecules [10] is selectively higher in NSCs than in neural precursor cells. These properties can be exploited to enable live monitoring of neural stem cell activity and prospective identification and isolation of NSCs by means of reporter genes made to express green fluorescence protein (GFP) by using the promoter or enhancer region of this group of genes [11]. In the present study, we would like to describe the process that led to the discovery of the neural stem/progenitor cell marker Musashi-1, which is regarded as having greatly contributed to stem-cell biology, not only as a marker, but because it has provided insights into the role of post-transcriptional gene regulation in the maintenance of stem cells.

Discovery and analysis of the function of the Drosophila MUSASHI gene

Musashi-1 is an RNA-binding protein family that is strongly expressed in the nervous system [12] and whose primary structure and expression pattern have been conserved among species in nematodes (*C. elegans*) [13], the fruit fly (*Drosophila*) [14,15], ascidians (*Ciona intestinalis*) [16], and in vertebrates as a whole [5,17]. Based on the loss-of-function phenotypes of the *musashi* gene in *Drosophila*, this gene was shown to play an essential role in the for asymmetrical division of sensory organ precursor cells (SOPs), which are precursor cells of the ectodermal system that are common to both neural and non-neural cell lineages. In wild-type *Drosophila*, each SOP normally gives rise to one IIa cell (non-neural precursor), which is an intermediate precursor cell, and one IIb cell (neural precursor), whereas in *musashi* mutants, SOPs are incapable of dividing asymmetrically, and two IIa cells are produced instead. As a result, the neural lineage derived from IIb cells that originally should have produced neural cells, such as neurons and glia, undergoes phenotypic transformation to hair-forming cells and socket-forming cells as support cells, which are IIa-cell-derived non-neural lineage cells, resulting in double-bristle phenotype with two hairs. The name MUSASHI, which refers to "bearing two swords", is derived from this double-bristle phenotype [12,14,18].

We were later able to clarify the regulatory mechanism of the asymmetric cell division of SOPs by the Musashi gene product of *Drosophila*. Starting with the conclusion, the Musashi gene product, which is an RNA-binding protein, was found to induce differentiation of IIb cells as neural precursor cells by selectively repressing translation of the mRNA of the neural differentiation inhibitory factor (a transcription repressor possessing a BTB domain and zinc-finger domain) called Tramtrack69 (TTK69) in IIb cells alone. In other words, although transcription of the *ttk69* gene actually occurs with similar efficiency in both IIa cells and IIb cells, translation of its mRNA in IIb cells is repressed by Musashi protein. TTK69 protein is expressed in IIa cells alone, and as a result it represses differentiation of IIa cells into neural precursor cells. The discovery that modulation of gene expression at the translation level regulates asymmetrical division is considered extremely interesting. However, in the early 1990s, when identification of the *musashi* gene was first reported, functional analysis of RNA-binding proteins had not yet been established. Identification of the RNA sequence and gene that was the target of the Musashi protein was absolutely essential to achieving a breakthrough. After spending several years establishing the conditions, we succeeded in identifying the RNA base sequence that is the binding-target of Musashi protein, which possesses two RNA-binding motifs, by using the in vitro selection method (SELEX method). More specifically, we chemically synthesized a DNA template (5′-GGGAAGATCTCGACCAGAAG-N_{50}-TATGTG-CGTCTACATGGATCCTCA-3′) with the T7 RNA polymerase recognition sequence attached at the 5′ end of a random DNA oligomer and the primer sequence for the reverse transcription by reverse polymerase at the 3′ end, and then prepared random-sequence RNA (random RNA pool) in a test tube by adding T7 RNA polymerase. Then, we added purified GST–Musashi fusion protein to a random RNA pool, and used a Glutathione–Sepharose 4Bs affinity column to isolate only the RNA molecule that binds to the GST–Musashi fusion protein. We later synthesized the corresponding cDNA by reverse transcription, amplified it by PCR between the T7 RNA polymerase recognition sequence and the primer sequence for reverse transcription, and then prepared template DNA for RNA synthesis. When this cycle was repeated 5 times, the RNA molecule that binds to the GST–Musashi fusion protein was highly

concentrated, and the cDNA of the RNA molecule that had been isolated was finally cloned and its base sequence was determined. The results revealed that Musashi protein binds to sequences that repeat (GUU•••UAG) or (GUU•••UG) 2 or 3 times (consensus sequence: GU_{3-5} (G or AG)) [19]. Interestingly, this sequence contributes to the asymmetric division of SOPs, and 15 sites are also present in the 3′ untranslated region (UTR) of *tramtrack69* (*ttk69*), which codes a repressor of neuronal differentiation. Although TTK69 protein is expressed in IIa support-cell precursor cells, it had been found not to be expressed in IIb neural precursor cells. Nevertheless, we demonstrated that *ttk69* mRNA is present in IIb neural precursor cells, despite the absence of expression of TTK69 protein [19]. This can be interpreted to mean that two IIa support-cell precursor cells emerge from the initial asymmetric division in *musashi* mutants, but the *ttk69* mRNA in the IIb neural precursor cell is translated into TTK69 protein, and as a result, two IIa support-cell precursor cells emerge. We therefore tested the hypothesis that Musashi protein represses translation of the mRNA by binding to the Musashi-protein-binding sequence of the 3′-UTR of *ttk69* mRNA. Interestingly, in a gain-of-function mutation of the *ttk* gene (ttk^1), a *Drosophila* transposon—P-element vector—was inserted within the exon corresponding to the 3′-UTR of *ttk69* mRNA [20]. As a result, the TTK69 protein was also translated in the IIb neural precursor cells of the ttk^1 mutant, as in the phenotype of the *musashi* mutant, and two IIa support-cell precursor cells were produced. This observation can be interpreted as showing that translational repression was eliminated because the Musashi protein was unable to act on the *ttk69* mRNA in the mutant, i.e., the *cis*-element for the translational repression of *ttk69* mRNA in IIb cells resides within the 3′-UTR of *ttk69* mRNA. Actually, in an in vitro experiment utilizing the chimeric Luciferase reporter gene, Musashi protein also repressed the translation of the Luciferase reporter gene through its effect on the 3′-UTR of *ttk69* mRNA. We therefore concluded that Musashi protein specifically binds to a binding sequence that is present on *ttk69* mRNA, and by repressing translation to TTK69 protein, which is a repressor of neuronal differentiation, maintains the potential of IIb neural precursor cells for neural differentiation. *Drosophila* Musashi protein is widely expressed in the compound eye primordium [15] and CNS [14]. It contributes to gene expression at the post-transcription level, i.e., to translation, etc., and it is predicted to possess a variety of context-dependent functions. Investigating whether *ttk69* mRNA is its sole target mRNA would seem to be an important future task.

Another puzzle remains, and that is that before and after SOP division, Musashi protein is almost equally distributed between the IIa cell and IIb cell. However, since Musashi protein only represses the translation of TTK69 protein in IIb neural precursor cells, repression of translation must not occur in IIa support-cell precursor cells despite the presence of Musashi protein [19]. We postulated that the function of Musashi protein in IIa cells is inactivated by modification at the post-translation level as a result of the actions of upstream signaling pathways. We are currently investigating the underlying mechanism.

The Musashi gene is also expressed in proliferating neural stem/progenitor cells (neuroblasts) [21] in the larval brain of *Drosophila* [14]. The neural stem/progenitor cells (neuroblasts) present in the larval brain differ from the neuroblasts in the embryonic development period, which only divide asymmetrically. After undergoing symmetric self-renewing division in the early stage, they have many characteristics in common with the mammalian NSCs in terms of repeated asymmetric divisions, and are considered a model system for mammalian neural stem/progenitor cells. Our research group is currently investigating the role of the Notch signal in these cells. We believe that the fact that Musashi is expressed in these cells is also important from the standpoint of considering the function of mammalian homologues of Musashi, which will be described next, and we have begun a functional analysis of Musashi in these cells. Overexpression of Musashi in the brain neural stem/progenitor cells of *Drosophila* larvae causes the proliferation of undifferentiated cells (Toriya M, Okano H; unpublished results). Thus, the role of *Drosophila* Musashi in larval neuroblasts may be analogous to that of mammalian Musashi-1, described below. Unlike the asymmetrical division of SOP, the phenomenon of induction of proliferation of neural stem/progenitor cells (neuroblasts) in the larval brain by overexpression of Musashi is difficult to explain by repression of translation of *ttk69* mRNA alone. A different function of Musashi due to a change in context is postulated, and we are currently conducting a genetic analysis in regard to this point. In the future, the Musashi and the Notch signaling systems in the neural stem/progenitor cells (neuroblasts) in larval brain are expected to contribute greatly as model systems to identification and analysis of factors that regulate the proliferation and differentiation of mammalian NSCs.

Musashi-1 as a marker of mammalian neural stem/progenitor cells, and its function

To elucidate the functions of the MUSASHI gene family in mammals, we first cloned the mouse homologue of Musashi-1 and then analyzed its pattern of expression in detail [5–7]. Based on the results of a series of studies on Musashi-1, we concluded that mammalian Musashi-1 plays important roles in cell fate decision, including the maintenance of the stem-cell state, differentiation, and tumorigenesis [12].

Musashi-1 is a member of the MUSASHI family in vertebrates, and analyses to date have shown that it is strongly expressed in the NSCs of the periventricular area or undifferentiated neural precursor cells of vertebrates as a whole. This has made it possible to map NSCs and progenitor cells in the CNS of a variety of vertebrates by

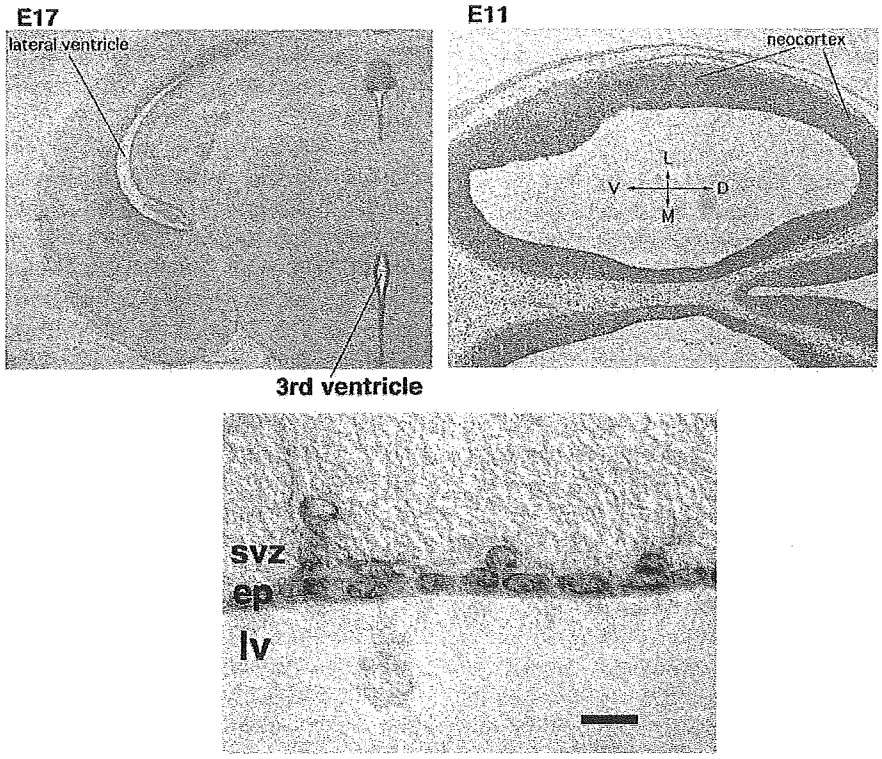

Fig. 1. Expression of Musashi-1 in mouse brain. Upper panel: Fetal forebrain (E17, E11). Lower panel: Adult forebrain (adapted from [7] with permission). In both fetal and adult stages, Musashi-1 protein is localized in the periventricular zone. Complete credit of the lower panel is given to the original source [7] and S. Karger AG, Basel.

using Musashi-1 as a marker. Our group in collaboration with Steven Goldman in the United States used Musashi-1 as a marker and succeeded in identifying NSCs and progenitor cells in the adult human brain [22].

A detailed analysis in the mouse has revealed strong expression of Musashi-1 in the ventricular zone of the neural tube in the embryo stage, when NSC and progenitor-cell division is very active in the CNS [5,7]. Strong expression of Musashi-1 protein has been observed at sites demonstrated in rodents, not only in the ventricular zone of the neural tube in the embryo stage, but also in the neurogenic sites within the postnatal brain including the so-called rostral migratory stream (RMS), which is a migration pathway from the external granule layer of the cerebellum and subventricular zone (SVZ) to the olfactory bulb [6]. In addition, the results of a detailed analysis have shown that Musashi-1 protein is selectively highly expressed in neural precursor cells, including NSCs, in the CNS during the embryonic stage (Fig. 1) [7]. The Musashi-1 protein in the postnatal CNS is expressed in the periventricular ependymal cells and astrocytes (SVZ astrocytes) (Fig. 1), which had been reported to possess stem cell characters in the adult brain [23,24]. Summarizing the above, expression of Musashi-1 protein in the CNS has been observed in NSCs around the ventricular zone of neural tube in the embryonic stage and in periventricular neural stem/progenitor cells (ependymal cells and SVZ astrocytes) in the adult. Thus, Musashi-1 protein has been confirmed to be continuously expressed in neural stem-cell-like cells. Because of this expression pattern, we have postulated that the RNA-binding protein Musashi-1 is not simply a marker, but is involved in regulating the properties of NSCs through regulation of the translation of specific mRNA. On the other hand, our research group has discovered a second MUSASHI gene in vertebrates and named it Musashi-2 [25]. Musashi-2 protein displays more than 90% homology with Musashi-1 protein at the amino acid level in the RNA-binding domain. Its pattern of expression in the CNS is also very similar to that of Musashi-1 in terms of being strongly expressed in neural stem/progenitor cells, and they have been postulated to play mutually overlapping roles (see below). Nevertheless, Musashi-2 differs in terms of being continuously expressed in only some of the neurons in the CNS and in its level of expression in organs outside the CNS being almost uniform [25]. A thorough analysis of Musashi-2 has only just begun, and we will describe only the results of the analysis centered on Musashi-1 below.

Functions of mammalian Musashi-1 protein

What sort of roles is mammalian Musashi-1 protein responsible for in NSCs? Musashi-1 protein has been found to function in cooperation with Musashi-2 protein to

activate Notch signaling through repression of translation of the mRNA of the intracellular Notch signal repressor m-Numb, and to maintain the self-renewing ability of NSCs. More specifically, before analyzing the functions of mammalian MUSASHI protein, as described above, we attempted to identify its target RNA sequence by the SELEX method, which we had used when we analyzed *Drosophila* Musashi [19], and we found that it sequence-specifically binds to RNA that possesses a sequence in which (G or A)U_nAGU [n = 1–3] is the motif [26]. When we searched for the mRNAs that possess this consensus sequence that are expressed in embryonic CNS, we confirmed that the Musashi-1 protein-binding sequence is present in the 3′-UTR of the *m-Numb* mRNA [27] and that Musashi-1 protein binds to *m-Numb* mRNA in vivo as well as in vitro. Musashi-1 protein was also shown to be present in the polysomal fraction [26], and was demonstrated to bind directly to a molecule that interacts with both a translation initiation factor and mRNA (Kawahara N, Imai T, Okano H; unpublished data), thereby repressing the target gene(s) at the translational level.

Based on the results of the analysis in *Drosophila*, m-Numb protein binds to the intracellular domain of Notch protein, and by guiding Notch protein endosomes from the cell surface and then to the degradation pathway, it is a modulator that exerts a repressive effect on the Notch signal [28]. Because m-Numb possesses such activity, it is thought that m-Numb protein positively modulates differentiation of neural stem/progenitor cells into neurons in the mammalian CNS, and that down-regulation of m-Numb protein itself from the neuron-production stage onward causes reactivation of the Notch signal and acts as the trigger for astroglia differentiation. Because it represses translation of this intracellular Notch-signal antagonist, Musashi-1 protein was expected to positively regulate Notch signaling, but actually it was confirmed that Musashi-1 protein induces transactivation of the promoter of the Notch signal target *Hes-1* gene [12,26]. In our previous study, we were able to demonstrate that overexpression of Musashi-1 induced the activation of Notch signaling through a pathway dependent on the action of CBF-1(RBP-J), which was measured by the transactivation of *Hes-1* promoter-Luciferase reporter, and the action of Musashi-1 to induce the transactivation of *Hes-1* promoter was found to be dependent on its RNA-binding activity [26].

It is now clear from a great deal of evidence that activation of the Notch signal positively regulates neural stem-cell self-renewal [29–31], and because it exerts an enhancing effect on the Notch signal, Musashi-1 is thought to contribute to retention of the properties of NSCs. We also demonstrated that the product of the second MUSASHI gene, Musashi-2, possesses *m-Numb* mRNA translation repressing activity, the same as Musashi-1 (Imai T and Okano H; unpublished data). Based on the pattern of expression described above as well, Musashi-2 has been postulated to act in the same manner as Musashi-1 in regulating NSCs.

When we combined preparation of knockout mice and functional repression by antisense ablation and conducted a functional double-knockout experiment on the Musashi-1 and Musashi-2 genes in order to elucidate this point, a sharp reduction in the efficiency of neurosphere formation was observed. By contrast, no such phenotype emerged as a result of single knockout (or knockdown) [32]. Thus, it appears that by functioning cooperatively, the Musashi-1 gene and Musashi-2 gene play important roles in maintaining the presence of NSCs or maintaining the undifferentiated state through repression of translation of *m-Numb* mRNA followed by activation of Notch signaling (Fig. 2) [12]. However, whether Musashi-1 and -2 proteins have target mRNA(s) other than *m-Numb* mRNA remains an open question. Future research study will elucidate the precise molecular mechanisms by which these mammalian MUSASHI proteins regulate the translation of their target mRNA(s), and their link to stem-cell maintenance.

Based on the above, although the target mRNA of the MUSASHI family differs in mammals and *Drosophila*, they both contribute to maintaining the character that produces neurons by regulating gene expression at the post-transcription level through repression of translation of target mRNA, and in that sense it seems that the function of the MUSASHI protein family can be said to have been conserved evolutionarily.

Musashi-1 as an epithelial stem-cell marker, and its significance

While it is true that the results of previous studies have shown that mammalian Musashi-1 increases the self-renewing ability of NSCs by activating Notch signaling through repression of translation of *m-Numb* mRNA, analysis of the upstream signal function involved in expression of the Musashi-1 gene is also important in terms of elucidating the full picture of stem cell regulation. The first step in elucidating it was to compare the Musashi-1 genes (including the base sequence of the 5′-upstream region and the intron region) in humans and mice, in both of which the base sequence of the entire genome has been deciphered, and to identify the sequences that have been conserved in both species. The results suggested that the Tcf/Lef binding sequence (Wnt signal response sequence) and Sox binding sequence are present in the regions that have been conserved outside the protein-coding region. The function of these sequences as transcription control *cis*-elements of the Musashi-1 gene is currently in the process of being analyzed. Wnt signaling and the Sox family transcription factors have each been found to play important roles in the induction and maintenance of intestinal stem cells, hematopoietic stem cells, certain types of neural stem/progenitor cells (Wnt signal: [33–35]), and undifferentiated neural precursor cells (Sox family: [21,22]). Based on what has already been learned, we set up a working hypothesis that expression of Musashi-1 is induced by Wnt signaling and the Sox family

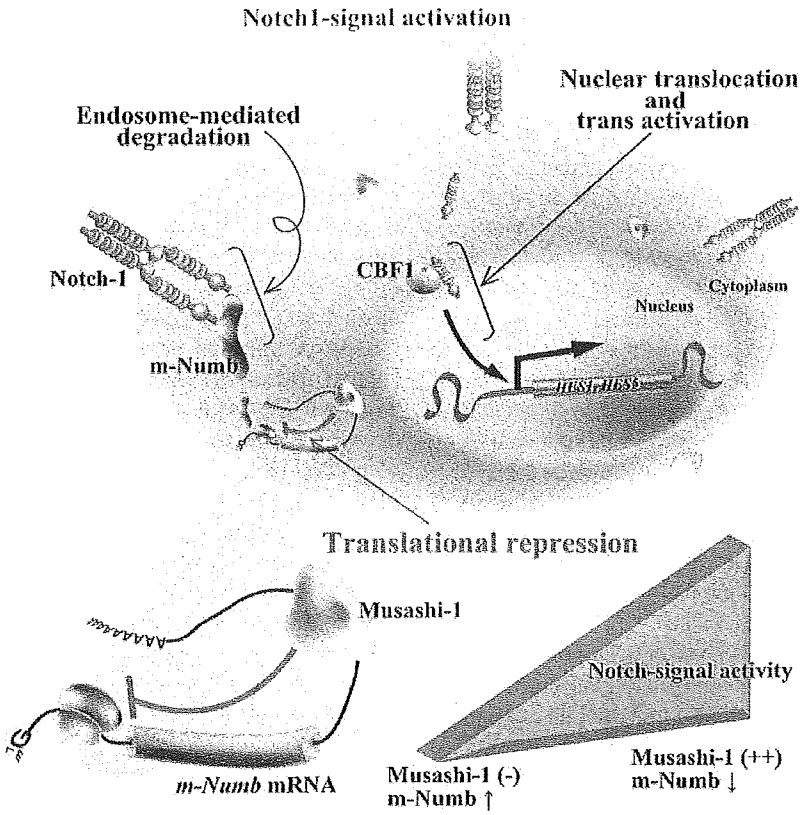

Fig. 2. Mechanism of Notch-1-signal activation by Musashi-1 protein. Musashi-1 protein binds to the 3′-UTR of *m-Numb* mRNA and inhibits its translation [26]. On the other hand, m-Numb protein binds to the intracellular domain of Notch-1 protein and inhibits the activation of the Notch-1 pathway, putatively by guiding Notch-1 protein from the cell surface to the endosome-mediated degradation pathway [28]. Consequently, Musashi-1 protein augments the Notch-1 signaling pathway. Through these mechanisms, Musashi-1 protein acts cooperatively with Musashi-2 protein to maintain the self-renewal of NSCs [12,32].

transcription factors, and that it then activates Notch signaling through repression of translation of *m-Numb* mRNA and causes crosstalk between several signal systems involved in the self-renewal of stem cells, and we are currently in the process of testing it. In the future, this Musashi-1 regulatory system may become an important target for screening for low-molecular-mass compounds that cause activation of endogenous NSCs described below.Assuming that it plays the general role of crosstalk with the signal systems involved in maintaining stem cells, Musashi-1 may contribute to maintaining stem-cell systems other than NSCs. When we reviewed the data from the Northern blot analysis we had performed previously, we noticed that the distribution of *musashi-1* mRNA in various organs other than the CNS was high in the small intestine of the adult [5]. Since Musashi-1 is expressed in the crypts, which is where intestinal epithelial stem cells are said to be present, we think that this may represent expression of Musashi-1 in intestinal epithelial stem cells and not a contribution by intestinal ganglion cells. To investigate this, we conducted a joint study with the epithelial stem-cell specialists Christopher Potten and Robert Clarke in the UK and discovered that Musashi-1 is also a marker of intestinal epithelial stem cells [36] and mammary stem cells [37]. The epithelial cells of intestinal villi of the small intestinal mucosa are replaced within 2–3 days, and this rapid cell turnover, in addition to self-renewal by the intestinal epithelial stem cells present in the crypts of the small intestine, is thought to be maintained by a continuous supply of precursor cells that produce four types of cells that compose the epithelium of the mucosa of the small intestine: enterocytes, goblet cells, entero-endocrine cells, and Paneth cells. In the small intestine, he observed expression of Musashi-1 in the cells up to the 4th–6th position from the bottom of the crypts (especially the 4th), and in the cells in the deepest portion of the large intestine, where the possibility of stem cells is considered to be high [38], suggesting that it can be used as a stem cell marker, especially in the epithelium of the mucosa of the small intestine [36]. The Wnt signal system is known to play an important role in maintaining epithelial stem cells in the intestine [38], and it has been suggested that nuclear localization of stabilized β-catenin reaches its highest level as a result of activation of the canonical pathway of the Wnt signal in the 4th cells from the bottom of the crypts, which is the stem-cell position [38,39]. The fact that expression of Musashi-1 increases in the intestinal epithelium of mutants with functional deficiency of the APC molecule, which constitutively activates the Wnt signal, suggested that the

Wnt signal path performs an important function in expression of Musashi-1 in intestinal epithelial stem cells. Interestingly, a downstream factor of the Notch signal, HES-1 protein, has been found to be expressed in intestinal epithelial stem cells that express Musashi-1 [40]. In other words, the Wnt signal pathway and the Notch signal pathway become activated simultaneously in intestinal epithelial stem cells, and we are currently investigating the biological significance of this phenomenon and whether Musashi-1 is responsible for the simultaneous activation of the two signals by analyzing knockout mice. In addition, as stated above, Musashi-1 is also expressed in mammary epithelial stem cells. The report of Hans Clevers et al. in the past suggested that Tcf-4, a transcription factor that functions in the canonical pathways of the Wnt signal, plays an important role in the stem cells of the mammary epithelium as well as the intestine [41]. This is very interesting in terms of the transcription repression of the Musashi-1 gene, which contains many Tcf binding consensus sequences in its 5′-upstream region, which has been conserved among species, and we are in the process of verifying its role in maintenance of the integrated Wnt > Tcf-4 > Musashi-1> Notch signal pathway in epithelial stem cells by analyzing stem cell dynamics in knockout mice for associated molecules. Thus, Musashi has begun to attract attention as a regulatory molecule that is also a marker of epithelial stem cells, in addition to NSCs.

Acknowledgments

We would like to thank Drs. Makoto Nakamura, Craig Montell, Shin-ichi Sakakibara, and Masataka Okabe for their contributions to the original research on Musashi and the members of the Okano Laboratory for their valuable discussions. This work was supported by grants from the Japanese Ministry of Education, Sports and Culture of Japan to HO, and a grant from the 21st Century COE program of the Ministry of Education, Science and Culture of Japan to Keio University.

References

[1] M. Loeffler, C.S. Potten, Stem cells and cellular pedigrees—A conceptual introduction, in: C.S. Potten (Ed.), Stem Cells, Acdemic Press Ltd, 1997, pp. 1–27.
[2] H. Okano, Making and repairing the mammalian brain: introduction, Semin. Cell Dev. Biol. 14 (2003) 159.
[3] H. Okano, The stem cell biology of the central nervous system, J. Neurosci. Res. 69 (2002) 698–707.
[4] H. Okano, Neural stem cells: progression of basic research and perspective for clinical application, Keio J. Med. 51 (2002) 115–128.
[5] S. Sakakibara, T. Imai, J. Aruga, K. Nakajima, D. Yasutomi, T. Nagata, Y. Kurihara, S. Uesugi, T. Miyata, M. Ogawa, K. Mikoshiba, H. Okano, Mouse-Musashi-1, a neural RNA-binding protein highly enriched in the mammalian CNS stem cell, Dev. Biol. 176 (1996) 230–242.
[6] S. Sakakibara, H. Okano, Expression of neural RNA-binding proteins in the post-natal CNS: implication of their roles in neural and glial cells development, J. Neurosci. 17 (1997) 8300–8312.
[7] Y. Kaneko, S. Sakakibara, T. Imai, A. Suzuki, Y. Nakamura, K. Sawamoto, Y. Ogawa, Y. Toyama, T. Miyata, H. Okano, Musashi1: an evolutionally conserved marker for CNS progenitor cells including neural stem cells, Dev. Neurosci. 22 (2000) 139–153.
[8] S. Hockfield, R.D. McKay, Identification of major cell classes in the developing mammalian nervous system, J Neurosci. 5 (1985) 3310–3328.
[9] U. Lendahl, L.B. Zimmerman, R.D.G. McKay, CNS stem cells express a new class of intermediate filament protein, Cell 60 (1990) 585–595.
[10] Y. Kamachi, M. Uchikawa, H. Kondoh, Pairing SOX off: with partners in the regulation of embryonic development, Trends Genet. 16 (2000) 182–187.
[11] A. Kawaguchi, T. Miyata, K. Sawamoto, N. Takashita, A. Murayama, W. Akamatsu, M. Ogawa, M. Okabe, Y. Tano, S.A. Goldman, H. Okano, Nestin-EGFP transgenic mice: visualization of the self-renewal and multipotency of CNS stem cells, Mol. Cell. Neurosci. 17 (2001) 259–273.
[12] H. Okano, T. Imai, M. Okabe, Musashi: a translational regulator of cell fates, J. Cell Sci. 115 (2002) 1355–1359.
[13] A. Yoda, H. Sawa, H. Okano, MSI-1, a neural RNA-binding protein, is involved in the male mating behavior in *Caenorhabditis elegans*, Genes Cells 5 (2000) 885–895.
[14] M. Nakamura, H. Okano, J. Blendy, C. Montell, MUSASHI, a neural RNA-binding protein required for *Drosophila* adult external sensory organ development, Neuron 13 (1994) 67–81.
[15] Y. Hirota, M. Okabe, T. Imai, M. Kurusu, A. Yamamoto, S. Miyao, M. Nakamura, K. Sawamoto, H. Okano, Musashi and Seven in absentia downregulate Tramtrack through distinct mechanisms in *Drosophila* eye development, Mech. Dev. 87 (1999) 93–101.
[16] T. Kawashima, A.R. Murakami, M. Ogasawara, K.J. Tanaka, R. Isoda, Y. Sasakura, T. Nishikata, H. Okano, K.W. Makabe, Expression patterns of musashi homologues of the ascidians, *Halocynthia roretzi* and *Ciona intestinalis*, Dev. Gene Evol. 210 (2000) 162–165.
[17] P. Good, A. Yoda, S. Sakakibara, A. Yamamoto, T. Imai, H. Sawa, T. Ikeuchi, S. Tsuji, H. Satoh, H. Okano, The Human Musashi homolog1 (MSI1) gene encoding the homologue of Musashi/Nrp-1, a neural RNA-binding protein putatively expressed in CNS stem cells and neural progenitor cells, Genomics 52 (1998) 382–384.
[18] E. Yoshikawa, Musashi, Kohdansha International, New York, 1981.
[19] M. Okabe, T. Imai, M. Kurusu, Y. Hiromi, H. Okano, Translational repression determines a neuronal potential in *Drosophila* asymmetric cell division, Nature 411 (2001) 94–98.
[20] W.C. Xiong, C. Montell, tramtrack is a transcriptional repressor required for cell fate determination in the *Drosophila* eye, Genes Dev. 7 (1993) 1085–1096.
[21] K. Ito, Y. Hotta, Proliferation pattern of postembryonic neuroblasts in the brain of *Drosophila melanogaster*, Dev. Biol. 149 (1992) 134–148.
[22] D.W. Pincus, H. Keyoung, C. Restelli, R.R. Goodman, R.A.R. Fraser, M. Edgar, S. Sakakibara, H. Okano, M. Nedergaard, S.A. Goldman, FGF2/BDNF-responsive neuronal progenitor cells in the adult human subependyma, Ann. Neurol. 43 (1998) 576–585.
[23] C.B. Johansson, S. Momma, D.L. Clarke, M. Risling, U. Lendahl, J. Frisen, Identification of a neural stem cell in the adult mammalian central nervous system, Cell 96 (1999) 25–34.
[24] F. Doetsch, I. Caille, D.A. Lim, J.M. Garcia-Verdugo, A. Alvarez-Buylla, Subventricular zone astrocytes are neural stem cells in the adult mammalian brain, Cell 97 (1999) 703–716.
[25] S. Sakakibara, Y. Nakamura, H. Satoh, H. Okano, RNA-binding protein Musashi2: developmentally regulated expression in neural precursor cells and subpopulation of neurons in mammalian CNS, J. Neurosci. 21 (2001) 8097–8107.

[26] T. Imai, A. Tokunaga, T. Yoshida, M. Hashimoto, G. Weinmaster, K. Mikoshiba, M. Nakafuku, H. Okano, The neural RNA-binding protein Musashi1 translationally regulates the m-numb gene expression by interacting with its mRNA, Mol. Cell. Biol. 21 (2001) 3888–39000.
[27] W. Zhong, J.N. Feder, M.M. Jiang, L.Y. Jan, Y.N. Jan, Asymmetric localization of a mammalian numb homolog during mouse cortical neurogenesis, Neuron 17 (1996) 43–53.
[28] D. Berdnik, T. Torok, M. Gonzalez-Gaitan, J.A. Knoblich, The endocytic protein alpha-Adaptin is required for numb-mediated asymmetric cell division in *Drosophila*, Dev. Cell. 3 (2002) 221–231.
[29] Y. Nakamura, S. Sakakibara, T. Miyata, M. Ogawa, T. Shimazaki, S. Weiss, R. Kageyama, H. Okano, The bHLH gene Hes1 as a repressor of neuronal commitment of the CNS stem cells, J. Neurosci. 20 (2000) 283–293.
[30] S. Hitoshi, T. Alexson, V. Tropepe, D. Donoviel, A.J. Elia, J.S. Nye, R.A. Conlon, T.W. Mak, A. Bernstein, D. van der Kooy, Notch pathway molecules are essential for the maintenance, but not the generation, of mammalian neural stem cells, Genes Dev. 16 (2002) 846–858.
[31] A. Tokunaga, J. Kohyama, T. Yoshida, K. Nakao, K. Sawamoto, H. Okano, Mapping spatio-temporal activation of Notch signaling during neurogenesis and gliogenesis in the developing mouse brain, J. Neurochem. 90 (2004) 142–154.
[32] S. Sakakibara, Y. Nakamura, M. Koike, H. Takano, Y. Uchiyama, T. Noda, H. Okano, RNA-binding protein Musashi family, roles for CNS stem cells and a subpopulation of ependymal cells revealed by targeted disruption and antisense ablation, Proc. Natl. Acad. Sci. U. S. A. 99 (2002) 15194–15199.
[33] V. Korinek, N. Barker, P. Moerer, E. van Donselaar, G. Huls, P.J. Peters, H. Clevers, Depletion of epithelial stem-cell compartments in the small intestine of mice lacking Tcf-4, Nat. Genet. 19 (1998) 379–383.
[34] T. Reya, A.W. Duncan, L. Ailles, J. Domen, D.C. Scherer, K. Willert, L. Hintz, R. Nusse, I.L. Weissman, A role for Wnt signalling in self-renewal of haematopoietic stem cells, Nature 22 (423) (2003) 409–414.
[35] S.M. Lee, S. Tole, E. Grove, A.P. McMahon, A local Wnt-3a signal is required for development of the mammalian hippocampus, Development 127 (2000) 457–467.
[36] C.S. Potten, C. Booth, G.L. Tudor, D. Booth, G. Brady, P. Hurley, G. Ashton, G. Clarke, S. Sakakibara, H. Okano, Identification of a putative intestinal stem cell marker and early lineage marker; Musashi1, Differentiation 71 (2003) 28–41.
[37] R.B. Clarke, K. Spence, E. Anderson, A. Howell, H. Okano, C.S. Potten, A putative human breast stem cell population is enriched for steroid receptor-positive cells, Dev. Biol. 277 (2005) 443–456.
[38] E. Marshman, C. Booth, C.S. Potten, The intestinal epithelial stem cell, BioEssays 24 (2002) 91–98.
[39] T. Kayahara, M. Sawada, S. Takaishi, H. Fukui, H. Seno, H. Fukuzawa, K. Suzuki, H. Hiai, R. Kageyama, H. Okano, T. Chiba, Candidate markers for stem and early progenitor cells, Musashi-1 and Hes1, are expressed in crypt base columnar cells of mouse small intestine, FEBS Lett. 535 (2003) 131–135.
[40] T. Sakatani, A. Kaneda, C.A. Iacobuzio-Donahue, M.G. Carter, S.B. Witzel, H. Okano, M.S.H. Ko, R. Ohlsson, D.L. Longo, A.P. Feinberg, Loss of imprinting of Igf2 alter intestinal maturation and tumorigenesis in mice. Science, in press.
[41] N. Barker, G. Huls, V. Korinek, H. Clevers, Restricted high level expression of Tcf-4 protein in intestinal and mammary gland epithelium, Am. J. Pathol. 154 (1999) 29–35.

Available online at www.sciencedirect.com
SCIENCE DIRECT®
Biochemical and Biophysical Research Communications 328 (2005) 348–352
BBRC
www.elsevier.com/locate/ybbrc

Hes1-deficient mice show precocious differentiation of Paneth cells in the small intestine☆

Katsumasa Suzuki[a], Hirokazu Fukui[a], Takahisa Kayahara[a], Mitsutaka Sawada[a], Hiroshi Seno[a], Hiroshi Hiai[b], Ryoichiro Kageyama[c], Hideyuki Okano[d], Tsutomu Chiba[a,*]

[a] *Department of Gastroenterology and Hepatology, Kyoto University Graduate School of Medicine, Kyoto, Japan*
[b] *Department of Pathology, Kyoto University Graduate School of Medicine, Kyoto, Japan*
[c] *Institute of Virus Research, Kyoto University Graduate School of Medicine, Kyoto, Japan*
[d] *Department of Physiology, Keio University School of Medicine, Tokyo, Japan*

Received 21 December 2004
Available online 7 January 2005

Abstract

We have previously shown that Hes1 is expressed both in putative epithelial stem cells just above Paneth cells and in the crypt base columnar cells between Paneth cells, while Hes1 is completely absent in Paneth cells. This study was undertaken to clarify the role of Hes1 in Paneth cell differentiation, using *Hes1*-knockout (KO) newborn (P0) mice. Electron microscopy revealed premature appearance of distinct cells containing cytoplasmic granules in the intervillous region in *Hes1*-KO P0 mice, whereas those cells were absent in wild-type (WT) P0 mice. In *Hes1*-KO P0 mice, the gene expressions of cryptdins, exclusively present in Paneth cells, were all enhanced compared with WT P0 mice. Immunohistochemistry demonstrated increased number of both lysozyme-positive and cryptdin-4-positive cells in the small intestinal epithelium of *Hes1*-KO P0 mice as compared to WT P0 mice. Thus, Hes1 appears to have an inhibitory role in Paneth cell differentiation in the small intestine.

Keywords: Hes1; Cryptdin; Musashi-1; Small intestine; Stem cell; Paneth cell

The small intestinal epithelium is characterized by continuous replacement of epithelial cells through proliferation and differentiation of a pool of progenitor cells throughout life. However, the exact mechanism of differentiation of small intestinal epithelium remains unclear. The epithelium of the small intestine is composed of four major types of cells: enterocytes, goblet cells, enteroendocrine cells, and Paneth cells. Although the former three types complete their differentiation during upward migration toward the villous tip, Paneth cells achieve their terminal differentiation as they migrate downwards to the crypt base [1–3].

Hes1, a transcriptional factor regulated by Notch signaling [4], is essential for the self-renewal activity of neural stem cells and for repression of their commitment to the neuronal lineage [5,6]. Recently, Jensen et al. [7] have reported that *Hes1*-deficient mice display excessive differentiation of multiple endocrine cell types in the developing small intestine, suggesting that, similar to its effect on neuronal differentiation, Hes1 may be involved in the inhibition of small intestinal cell differentiation toward endocrine cells. Interestingly, we have recently shown that Hes1 is co-localized with Musashi-1, a possible stem cell marker of small intestinal epithelial cells, in a few cells just above Paneth cells (putative stem cells), and

☆ This work was supported in part by Grants-in-Aid from the Ministry of Education, Culture, Sports, Science and Technology, Japan.
☆☆ *Abbreviations:* KO, knockout; WT, wild-type; RT-PCR, reverse transcription-polymerase chain reaction; GAPDH, glyceraldehyde-3-phosphate dehydrogenase.
* Corresponding author. Fax: +81 75 751 4303.
E-mail address: cteya@kuhp.kyoto-u.ac.jp (T. Chiba).

0006-291X/$ - see front matter © 2005 Elsevier Inc. All rights reserved.
doi:10.1016/j.bbrc.2004.12.174

in crypt base columnar cells located between Paneth cells [8], suggesting involvement of Hes1 in Paneth cell differentiation as well as maintenance of stem cells. In the present study, therefore, by using *Hes1*-knockout (KO) mice, we tried to elucidate the role of Hes1 in Paneth cell differentiation.

Materials and methods

Animals. Pregnant CD1-*Hes1* mice [9] were kept in isolator cages in a barrier facility under a 12 h light cycle and maintained under specific pathogen-free conditions. *Hes1*-double KO mice die immediately after birth. Therefore, for the study, we sacrificed the *Hes1*-KO and wild-type (WT) newborn (P0) mice immediately after birth. *Hes1*-KO mice were genotyped as reported previously [9]. All animal procedures followed the guidelines for animal experiment of Kyoto University.

Electron microscopy. After P0 mice had been sacrificed, their small intestines were immediately fixed in 1% glutaraldehyde and 1.4% paraformaldehyde in 0.1 M phosphate buffer (pH 7.2), postfixed in 1% osmium tetroxide in 0.1 M phosphate buffer, dehydrated in a graded ethanol series, and embedded in Epon resin. After staining with uranyl acetate and lead citrate, the ultrathin sections were examined under an electron microscope (Hitachi H-700, Tokyo) [10].

RNA extraction and reverse transcription-polymerase chain reaction (RT-PCR). Total RNA was extracted using the single-step guanidinium thiocyanate–phenol–chloroform method (Trizol; Gibco-BRL). To generate cDNA, 5 μg of total RNA was reverse-transcribed using 200 U SuperScript II RT (Gibco-BRL) in a total reaction volume of 20 μl. For the following PCR, pairs of oligonucleotide primers for mouse *cryptdin-1*, *cryptdin-4*, and *cryptdin-5*, mouse *lysozyme*, and mouse *glyceraldehyde-3-phosphate dehydrogenase* (*GAPDH*) were prepared: mouse *cryptdin-1*, *-4*, and *-5*, 5′-AAGAGACTAAAACTGAGGAGCAGC-3′ (sense) and 5′-CGACAGCAGAGCGTGTA-3′ (*cryptdin-1*; antisense), 5′-CGGCGGGGGCAGCAGTA-3′ (*cryptdin-4*; antisense), or 5′-GCA GCAGAATACGAAAGT-3′ (*cryptdin-5*; antisense) [11]; mouse *lysozyme* 5′-GGTCTACAATCGTTGTGAGTTGG-3′ (sense) and 5′-CTC CGCAGTTCCGAATATACTT-3′ (antisense); and mouse *GAPDH*, 5′-TTAGCCCCCCTGGCCAAGG-3′ (sense) and 5′-CTTACTCCTT GGAGGCCATG-3′ (antisense).

One microliter of reverse-transcription product was amplified by PCR in a 50 μl reaction volume containing 10 pmol of the above primer sets, 1.25 U Ampli-*Taq* DNA polymerase (Applied Biosystems, Branchburg, NJ, USA), PCR buffer [final concentration: 20 mM Tris–HCl (pH 8.4), 50 mM KCl], 2.5 mM $MgCl_2$, 10 mM dithiothreitol, and 1 mM dNTP. The PCR amplification was performed as follows: 95 °C for 10 min, 40, 35, 30, 25, 20, or 15 cycles of 94 °C for 30 s, 55 °C for 30 s, and 72 °C for 1 min, with a final extension step of 72 °C for 5 min.

Immunohistochemistry. The small intestine removed from ICR mice was fixed with 4% paraformaldehyde overnight in 0.1 M phosphate-buffered saline (PBS; pH 7.4) at 4 °C, embedded in paraffin and OCT compound (Tissue-Tek; Sakura Finetechnical, Tokyo, Japan), and cut perpendicularly at a thickness of 6 μm. Immunostaining for Musashi-1, Hes1, Lysozyme, Cryptdin-4, and Ki-67, a proliferation marker, was performed as described previously [8,12,13]. In brief, sections were treated with 3% H_2O_2 in methanol for 20 min to quench endogenous peroxidase activity. The sections were then placed in 0.01 M citrate buffer (pH 6.0) and treated with microwave heating for 10 min to facilitate antigen retrieval. The sections were immunostained using a Vectastain ABC kit (Vector Laboratories, Burlingame, CA, USA) according to the manufacturer's instructions. Sections were incubated with 3% bovine serum albumin in PBS for 30 min and then incubated with anti-Musashi-1 antibody (final dilution 1:1000) [12], anti-Hes1 antibody (kindly supplied by Dr. T. Sudo, Toray Industries, Tokyo, Japan, final dilution 1:1000) [13], anti-lysozyme antibody (DAKO, Carpinteria, CA, USA, final dilution 1:200), anti-cryptdin-4 (α-defensin-4) antibody (Santa Cruz Biotechnology, CA, USA, final dilution 1:100) or anti-mouse Ki-67 antibody (Dako Cytomation, Copenhagen, Denmark; final dilution 1:200), according to the manufacturer's instructions, at 37 °C for 30 min. The sections were incubated with biotinylated secondary antibody for 40 min. After washing with PBS, avidin–biotin complex was applied for 30 min. The sections were then incubated in 3,3′-diaminobenzidine tetrahydrochloride with 0.05% H_2O_2 for 3 min and counterstained with Mayer's hematoxylin. To count the number of lysozyme-positive or cryptdin-4-positive cells, well-oriented areas from the villus to the intervillous region were selected. These positive cells were counted in at least 15 different areas from the villus to the intervillous region for each section, and the results were averaged.

Results

Lysozyme and cryptdin mRNA expressions in the small intestine of WT and Hes1-KO P0 mice

Lysozyme mRNA expression in the small intestine of *Hes1*-KO P0 mice was slightly increased compared with that of WT P0 mice. Moreover, in the small intestine of WT mice, only faint expression of *cryptdin-1*, *-4*, and *-5* mRNAs was observed at 35 cycles of PCR, whereas expression was greatly enhanced in *Hes1*-KO mice (Fig. 1).

Hes1, Musashi-1, lysozyme, and cryptdin-4 protein expression in the small intestine of WT and Hes1-KO P0 mice

A few Hes1-positive cells were present in the intervillous region of the small intestine of WT P0 mice, but no such cells could be detected in *Hes1*-KO mice (Fig. 2). On the other hand, Musashi-1 expression was observed in the cells located in the intervillous region of both *Hes1*-KO and WT P0 mice. However, the intensity of Musashi-1 immunoreactivity in *Hes1*-KO P0 mice was less than that in WT P0 mice (Fig. 2).

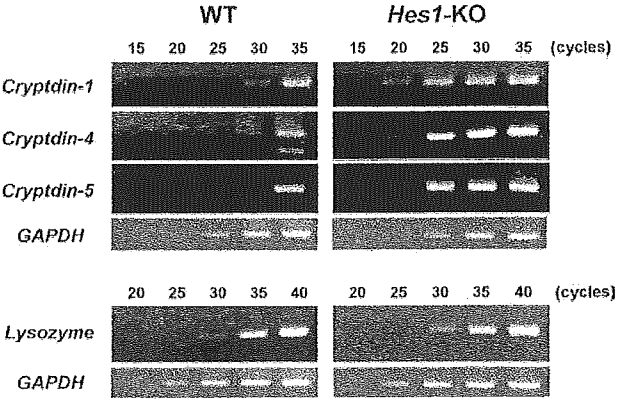

Fig. 1. *Lysozyme* and *cryptdin* mRNA expressions in the small intestine of WT and *Hes1*-newborn mice.

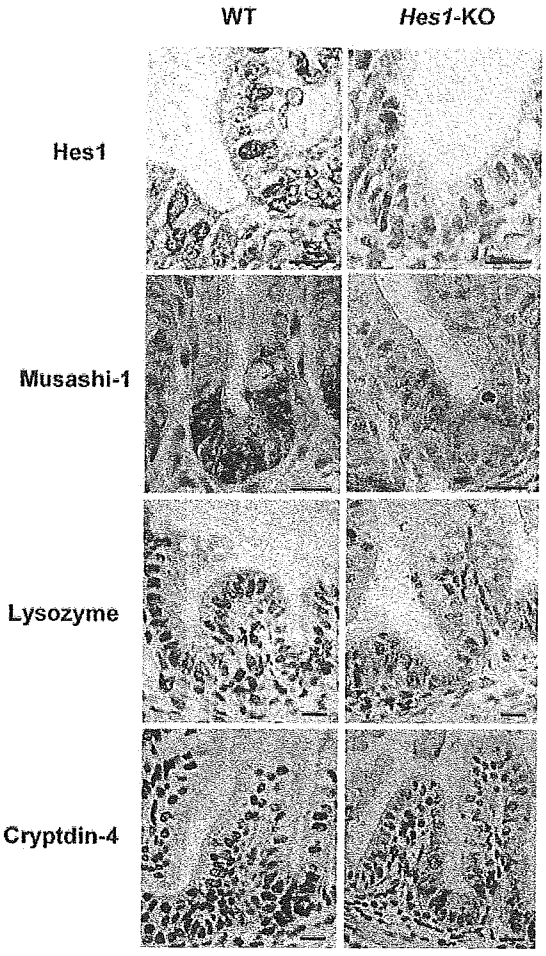

Fig. 2. Immunohistochemistry for Hes1 (bars = 10 μm), Musashi-1 (bars = 10 μm), lysozyme (bars = 10 μm), and cryptdin-4 (bars = 10 μm) in the small intestine of WT and *Hes1*-KO newborn mice.

Although lysozyme-positive and cryptdin-4-positive cells were hardly detected throughout the small intestinal epithelium of WT P0 mice, a few lysozyme-positive and cryptdin-4-positive cells were observed not only in the intervillous regions but also in the villi of *Hes1*-KO P0 mice (Fig. 2 and Table 1).

Electron microscopy

As in WT mice [8], there were no crypt structures in *Hes1*-KO mouse small intestine immediately after birth (P0). Normally, mature Paneth cells contain a large number of cytoplasmic granules. In WT P0 mice, we could hardly observe granule-containing cells throughout the small intestinal epithelium (Fig. 3A). In contrast, a few granule-containing cells could be detected in the villi or in the intervillous regions of *Hes1*-KO P0 mice (Fig. 3B). These granules contain high-density core matrix with low-density peripheral halo, resembling that of Paneth cells [14]. However, we usually observed immature Paneth cells with small granules, but hardly detected mature Paneth cells with large granules in *Hes1*-KO P0 mice. There were no obvious differences in the other cells in the intervillous region between *Hes1*-KO and WT mice.

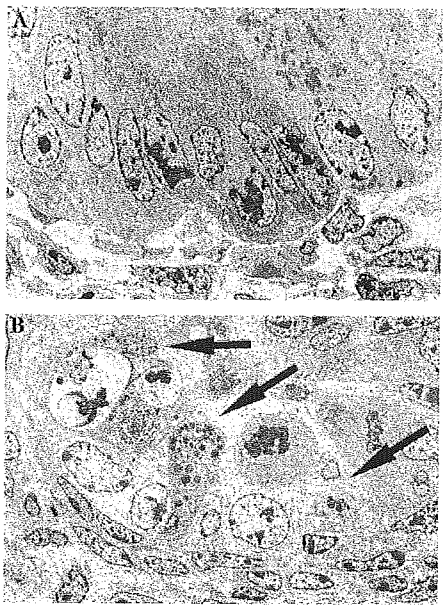

Fig. 3. Electron photomicrograph of the small intestine of a newborn WT mouse (A) and *Hes1*-KO newborn mouse (B). Granule-containing Paneth cells are observed in *Hes1*-KO newborn mouse (arrows in B), while no Paneth cells are seen in WT newborn mouse (bar = 2 μm).

Table 1
Number of lysozyme-positive and cryptdin-4-positive cells in the small intestine of WT and *Hes1*-KO newborn mice

	Lysozyme-positive cells		Cryptdin-4-positive cells	
	Villus	Intervillous region	Villus	Intervillous region
WT ($n = 4$)	0.00 ± 0.00	0.03 ± 0.02	0.00 ± 0.00	0.21 ± 0.07
Hes1-KO ($n = 8$)	$0.81 \pm 0.07^*$	$0.49 \pm 0.05^*$	$2.68 \pm 0.29^*$	$0.82 \pm 0.19^*$

The number of lysozyme-positive and cryptdin-4-positive cells was evaluated as described in Materials and methods. Results are expressed as means ± SE cells/each villus or intervillous region.

* Significantly greater than WT $P < 0.05$.

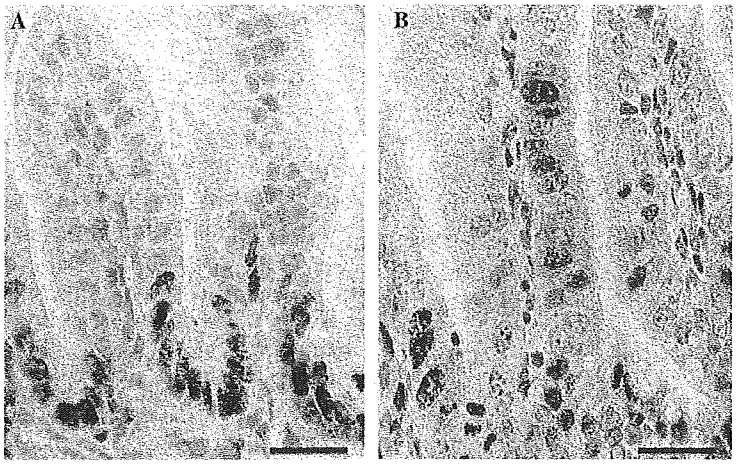

Fig. 4. Ki-67 expression in the small intestine of WT (A) and *Hes1*-KO (B) newborn mice (bars = 25 μm).

Ki-67 expression in the small intestine of WT and Hes1-KO P0 mice

In WT P0 mice, Ki-67-positive cells were present exclusively in the intervillous region of the small intestine, at a position corresponding to that of Hes1-positive cells. In contrast, in *Hes1*-KO P0 mice, Ki-67-positive cells were not localized to the intervillous region, but showed an irregular distribution throughout the epithelium (Fig. 4). This change was mirrored by a decrease in the number of Ki-67-positive cells in the intervillous region of *Hes1*-KO mice compared with WT P0 mice.

Discussion

We have shown previously that, in mouse small intestine, Hes1 is present in the nuclei of the cells just above Paneth cells (putative stem cells), and in crypt base columnar cells between Paneth cells, while Paneth cells are completely devoid of Hes1 staining, suggesting an inhibitory role for Hes1 in Paneth cell differentiation [8]. To further elucidate the role of Hes1 in Paneth cell differentiation, we used *Hes1*-KO newborn mice in this study. Previous studies have reported that no Paneth cells are present immediately after birth in normal mouse small intestine [8].

Electron microscopic observation in the present study revealed premature appearance of granule-containing cells, which resembled Paneth cells, in the small intestinal epithelium of *Hes1*-KO mice. In addition, we found that, in *Hes1*-KO mice, the gene expressions of cryptdins-1, -4, and -5, which are exclusively present in Paneth cells, were all enhanced compared with those in WT P0 mice. Furthermore, immunohistochemical studies demonstrated that, although lysozyme-positive and cryptdin-4-positive cells were hardly detected throughout the small intestinal epithelium of WT P0 mice, significant numbers of lysozyme-positive and cryptdin-4-positive cells were detected in the small intestinal epithelium of *Hes1*-KO P0 mice. These data confirmed precocious development of Paneth cells immediately after birth in *Hes1*-KO mice, suggesting that Hes1 has an inhibitory role in Paneth cell differentiation. Interestingly, we found in this study that lysozyme-positive and cryptdin-4-positive cells were detected not only in the intervillous regions but also in the villi of *Hes1*-KO P0 mice. These results may suggest that Hes1 also plays a role in the distribution of Paneth cells in the small intestinal epithelium.

Jensen et al. [7] have previously reported that *Hes1*-KO mice show precocious and excessive differentiation of multiple endocrine cell types in the small intestinal mucosa. Taken together, these findings indicate that Hes1 appears to act as a general negative regulator in differentiation of the small intestinal epithelium. Yang et al. [15] have shown that, in addition to disturbance of enteroendocrine and goblet cell development, development of Paneth cells is disturbed in *Math1*-deficient mice. Because Hes1 antagonizes the transcriptional activity of *Math1* [16], Hes1 may exert a general inhibitory action on differentiation of small intestinal cells, including Paneth cells, through antagonization of *Math1* transcriptional activity.

In this study, we observed that, in contrast to WT mice, Ki-67-positive cells in *Hes1*-KO newborn mice were not localized to the intervillous region, but were irregularly distributed throughout the epithelium. As strong Ki-67 staining is generally observed in proliferating progenitor cells in the intervillous region of normal newborn mice as well as in the crypt base of adult mice [8], our data may indicate that Hes1 has a role in localizing progenitor cells in the intervillous region or in the crypt base. Alternatively, precociously developed cells in

Hes1-KO mice, that have lost their proliferation activity, may have intermingled with Ki-67-positive progenitor cells.

We have previously shown that Musashi-1 is co-localized with Hes1 in the cells of the intervillous region of newborn mice [8]. Imai et al. [17] have reported that Musashi-1 enhances promoter activity of the *Hes1* gene. Our present study revealed that expression of Musashi-1 protein was decreased in *Hes1*-KO newborn mice. This suggests a positive feedback mechanism for Musashi-1 expression by Hes1, decelerating the differentiation process. Alternatively, as Musashi-1 is considered to be a stem cell marker in the small intestine [18], the decrease in Musashi-1-positive cells in *Hes1*-KO newborn mice may merely reflect a decrease of the stem cell pool by enhancement of precocious differentiation of the stem or progenitor cells in the intervillous region.

In summary, we have clearly demonstrated precocious development of Paneth cells in the small intestine of *Hes1*-deficient mice, indicating that Hes1 plays an inhibitory role in Paneth cell differentiation. It was noteworthy that, although crypt base columnar cells are strongly positive for Hes1, adjacent Paneth cells are completely devoid of Hes1. Thus, the mechanism of such sudden loss of Hes1 expression in crypt base columnar cells with resulting terminal differentiation toward Paneth cells needs to be elucidated in future studies.

Acknowledgments

We thank Dr. T. Sudo in Toray Industries, Tokyo, Japan, for kindly providing anti-Hes1 antibody. We also thank M. Fujioka (Central Laboratory for Electron Microscopy, Kyoto University Graduate School of Medicine) for technical assistance with the electron microscopy.

References

[1] H. Cheng, C.P. Leblond, Origin, differentiation and renewal of the four main epithelial cell types in the mouse small intestine. V. Unitarian Theory of the origin of the four epithelial cell types, Am. J. Anat. 141 (1974) 537–561.

[2] M. Bjerknes, H. Cheng, The stem-cell zone of the small intestinal epithelium. I. Evidence from Paneth cells in the adult mouse, Am. J. Anat. 160 (1981) 51–63.

[3] C. Booth, C.S. Potten, Gut instincts: thoughts on intestinal epithelial stem cells, J. Clin. Invest. 105 (2000) 1493–1499.

[4] S. Jarriault, C. Brou, F. Logeat, E.H. Schroeter, R. Kopan, A. Israel, Signalling downstream of activated mammalian Notch, Nature 377 (1995) 355–358.

[5] C. Akazawa, Y. Sasai, S. Nakanishi, R. Kageyama, Molecular characterization of a rat negative regulator with a basic helix–loop–helix structure predominantly expressed in the developing nervous system, J. Biol. Chem. 267 (1992) 21879–21885.

[6] Y. Sasai, R. Kageyama, Y. Tagawa, R. Shigemoto, S. Nakanishi, Two mammalian helix–loop–helix factors structurally related to *Drosophila* hairy and enhancer of split, Genes Dev. 6 (1992) 2620–2634.

[7] J. Jensen, E.E. Pedersen, P. Galante, J. Hald, R.S. Heller, M. Ishibashi, R. Kageyama, F. Guillemot, P. Serup, O.D. Madsen, Control of endodermal endocrine development by Hes-1, Nat. Genet. 24 (2000) 36–44.

[8] T. Kayahara, M. Sawada, S. Takaishi, H. Fukui, H. Seno, H. Fukuzawa, K. Suzuki, H. Hiai, R. Kageyama, H. Okano, T. Chiba, Candidate markers for stem and early progenitor cells, Musashi-1 and Hes1, are expressed in crypt base columnar cells of mouse small intestine, FEBS Lett. 535 (2003) 131–135.

[9] M. Ishibashi, S.L. Ang, K. Shiota, S. Nakanishi, R. Kageyama, F. Guillemot, Targeted disruption of mammalian hairy and enhancer of split homolog-1 (HES-1) leads to up-regulation of neural helix–loop–helix factors, premature neurogenesis, and severe neural tube defects, Genes Dev. 9 (1995) 3136–3148.

[10] M. Sawada, K. Takahashi, S. Sawada, O. Midorikawa, Selective killing of Paneth cells by intravenous administration of dithizone in rats, Int. J. Exp. Path. 72 (1991) 407–421.

[11] D. Darmoul, D. Brown, M. Selsted, A.J. Ouellette, Cryptdin gene expression in developing mouse small intestine, Am. J. Physiol. 272 (1997) G197–G206.

[12] Y. Kaneko, S. Sakakibara, T. Imai, A. Suzuki, Y. Nakamura, K. Sawamoto, Y. Ogawa, T. Miyata, H. Okano, Musashi1: an evolutionally conserved marker for CNS progenitor cells including neural stem cells, Dev. Neurosci. 22 (2000) 139–153.

[13] T. Ito, N. Udaka, T. Yazawa, K. Okudera, H. Hayashi, T. Sudo, F. Guillemot, R. Kageyama, H. Kitamura, Basic helix–loop–helix transcription factors regulate the neuroendocrine differentiation of fetal mouse pulmonary epithelium, Development 127 (2000) 3913–3921.

[14] A. Ahonen, Histochemical and electron microscopic observations on the development, neural control and function of the Paneth cells of the mouse, Acta Physiol. Scand. Suppl. 398 (1973) 1–71.

[15] Q. Yang, N.A. Bermingham, M.J. Finegold, H.Y. Zoghbl, Requirement of Math1 for secretory cell lineage commitment in the mouse intestine, Science 294 (2001) 2155–2158.

[16] C. Akazawa, M. Ishibashi, C. Shimizu, S. Nakanishi, R. Kageyama, A mammalian helix–loop–helix factor structurally related to the product of *Drosophila* proneural gene atonal is a positive transcriptional regulator expressed in the developing nervous system, J. Biol. Chem. 270 (1995) 8730–8738.

[17] T. Imai, A. Tokunaga, T. Yoshida, M. Hashimoto, K. Mikoshiba, G. Weinmaster, M. Nakafuku, H. Okano, The neural RNA-binding protein Musashi1 translationally regulates mammalian numb gene expression by interacting with its mRNA, Mol. Cell. Biol. 21 (2001) 3888–3900.

[18] C.S. Potten, C. Booth, G.L. Tudor, D. Booth, G. Brady, P. Hurley, G. Ashton, R. Clarke, S. Sakakibara, H. Okano, Identification of a putative intestinal stem cell and early lineage marker; musashi-1, Differentiation 71 (2003) 28–41.

Autoamplification of NFATc1 expression determines its essential role in bone homeostasis

Masataka Asagiri,[1,4,5] Kojiro Sato,[1,4,5] Takako Usami,[7] Sae Ochi,[1,2,4] Hiroshi Nishina,[8] Hiroki Yoshida,[6,9] Ikuo Morita,[3,4] Erwin F. Wagner,[10] Tak W. Mak,[11,12] Edgar Serfling,[13] and Hiroshi Takayanagi[1,4,5]

[1]Department of Cell Signaling [2]Department of Medicine and Rheumatology, [3]Department of Cellular Physiological Chemistry, Graduate School, and [4]Center of Excellence Program for Frontier Research on Molecular Destruction and Reconstruction of Tooth and Bone, Tokyo Medical and Dental University, Tokyo 113-8549, Japan
[5]Solution Oriented Research for Science and Technology and [6]Precursory Research for Embryonic Science and Technology, Japan Science and Technology Agency, Kawaguchi, Saitama 332-0012, Japan
[7]Laboratory of Recombinant Animals and [8]Department of Developmental and Regenerative Biology, Medical Research Institute, Tokyo Medical and Dental University, Tokyo 101-0062, Japan
[9]Department of Biomolecular Sciences, Faculty of Medicine, Saga University, Saga City, Saga 849-8501, Japan
[10]Research Institute of Molecular Pathology, A-1030 Vienna, Austria
[11]Ontario Cancer Institute, Princess Margaret Hospital, Toronto, Ontario M5G 2M9, Canada
[12]Department of Medical Biophysics, Advanced Medical Discovery Institute, University of Toronto, Toronto, Ontario M5G 2C1, Canada
[13]Department of Molecular Pathology, Institute of Pathology, University of Würzburg, D-97080 Würzburg, Germany

NFATc1 and NFATc2 are functionally redundant in the immune system, but it was suggested that NFATc1 is required exclusively for differentiation of osteoclasts in the skeletal system. Here we provide genetic evidence that *NFATc1* is essential for osteoclast differentiation in vivo by adoptive transfer of *NFATc1*$^{-/-}$ hematopoietic stem cells to osteoclast-deficient *Fos*$^{-/-}$ mice, and by *Fos*$^{-/-}$ blastocyst complementation, thus avoiding the embryonic lethality of *NFATc1*$^{-/-}$ mice. However, in vitro osteoclastogenesis in *NFATc1*-deficient cells was rescued by ectopic expression of NFATc2. The discrepancy between the in vivo essential role of *NFATc1* and the in vitro effect of NFATc2 was attributed to selective autoregulation of the *NFATc1* gene by NFAT through its promoter region. This suggested that an epigenetic mechanism contributes to the essential function of *NFATc1* in cell lineage commitment. Thus, this study establishes that *NFATc1* represents a potential therapeutic target for bone disease and reveals a mechanism that underlies the essential role of *NFATc1* in bone homeostasis.

CORRESPONDENCE
Hiroshi Takayanagi:
taka.csi@tmd.ac.jp

Abbreviations used: AP, activator protein; BMM, bone marrow monocyte/macrophage precursor cell; CBP, CREB-binding protein; ChIP, chromatin immunoprecipitation; ES, embryonic stem; FLC, fetal liver cell; MeCP2, methyl-CpG binding protein 2; RANKL, receptor activator of NF-κB ligand.

The mechanism underlying irreversible cell fate determination is critical for an understanding of biologic systems in vertebrates, where the NFAT family of transcription factors plays important roles (1, 2). Mice deficient in individual NFAT proteins exhibit a relatively mild phenotype in immune cells or neurons (1, 2), which suggests that the different family members play redundant roles in these systems (1–3). Homeostasis of the skeletal system depends on a balance between bone-forming osteoblasts and bone-resorbing osteoclasts (4). The critical role of *NFATc1* in the skeletal system was suggested by selective and strong induction of *NFATc1* in bone marrow monocyte/macrophage precursor cells (BMMs) that were stimulated with a key cytokine for osteoclastogenesis, receptor activator of NF-κB ligand (RANKL) (5, 6). Although our previous in vitro analyses indicated that NFATc1 is the essential transcription factor for osteoclast differentiation (5), little is known about its in vivo function in osteoclastogenesis because targeted disruption of the *NFATc1* gene in mice results in embryonic lethality. Furthermore, there is a contrasting report that NFATc2 also activates this process and may have a redundant role (7). Considering the close functional similarity of NFATc1 and NFATc2 (3, 7), it is important to determine whether *NFATc1* is essential for osteoclast differentiation in vivo, and, if so, how it exerts an indispensable function in this cell type.

In this report, we provide in vivo genetic evidence for the essential role of *NFATc1* by two novel techniques: adoptive transfer of hematopoietic stem cells to osteoclast-deficient

The online version of this article contains supplemental material.

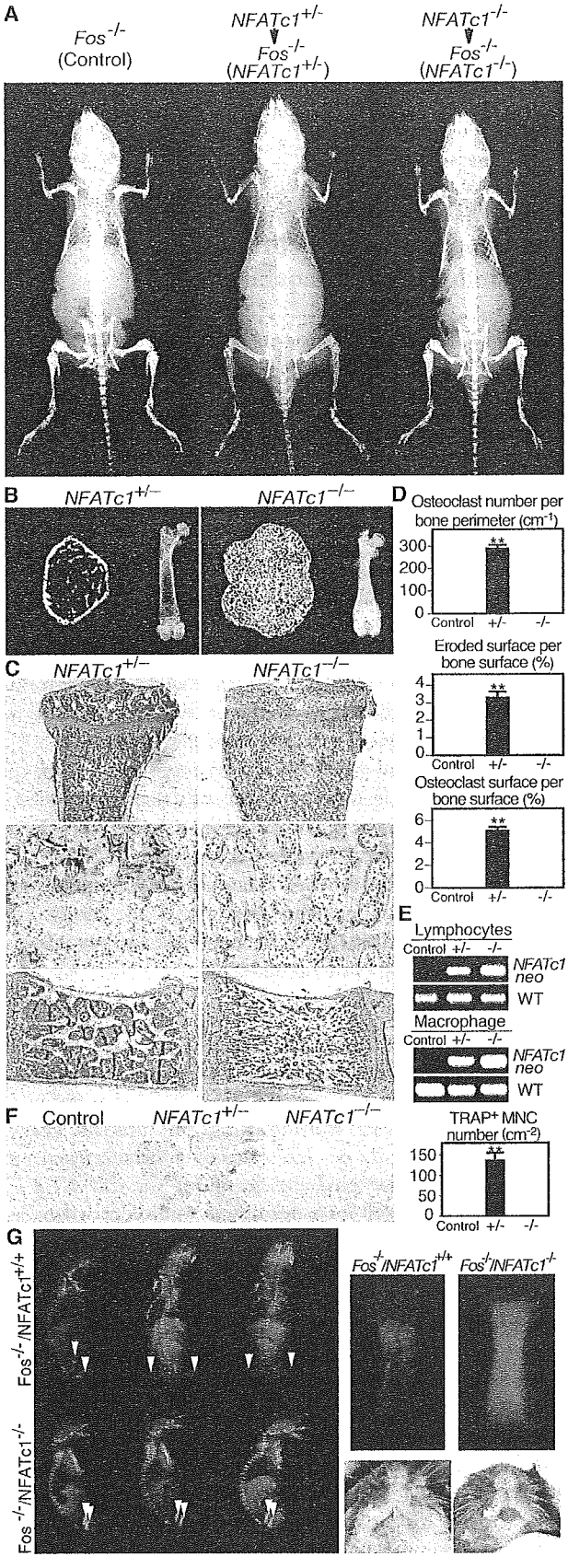

Fos$^{-/-}$ mice and *Fos*-deficient blastocyst complementation. *NFATc1*-deficient osteoclast precursor cells cannot differentiate into osteoclasts. Conversely, osteoclastogenesis of *NFATc1*-deficient cells is rescued by forced expression of NFATc2. The discrepancy between the essential role of *NFATc1* and the in vitro effect of NFATc2 is attributed to selective autoregulation of the *NFATc1* gene by NFAT through its promoter region. Our analysis indicates that the essential role of NFATc1 in bone homeostasis is not determined by its distinct biochemical properties, but is determined by its unique spatiotemporal activation mechanism during osteoclastogenesis.

RESULTS

In vivo evidence for the essential role of *NFATc1* in osteoclast differentiation shown by the fetal liver cell (FLC) transfer

Because in vivo analysis of the role of *NFATc1* has been hampered by embryonic lethality (8, 9), one may postulate that a conditional gene targeting strategy should be appropriate to avoid the difficulty. However, there is no desirable promoter to drive *cre* (encoding Cre recombinase) in the very early stage of osteoclast development. Adoptive transfer of hematopoietic stem cells to irradiated lymphocyte-deficient mice (10, 11) is used as an established method to analyze the function of such a gene in the study of lymphocytes (3). Here we applied this method to the skeletal system using mice lacking *c-Fos* (*Fos*$^{-/-}$ mice) (12, 13) as osteoclast-deficient recipients. Hematopoietic stem cells that were derived from *NFATc1*$^{+/-}$ and *NFATc1*$^{-/-}$ FLCs were injected into the liver of busulfan-treated newborn mice of *Fos*$^{-/-}$ background, in which no osteoclasts form because of a cell autonomous defect (13). Osteopetrosis is amelio-

Figure 1. In vivo evidence for the essential role of *NFATc1* in osteoclast differentiation. (A) Radiographic analysis of *Fos*$^{-/-}$ mice transferred with *NFATc1*$^{+/-}$ or *NFATc1*$^{-/-}$ FLCs. Severe osteopetrosis persists after *NFATc1*$^{-/-}$ FLC transfer. (B) Microradiographic analysis of femur (left: microcomputed tomography; right: microradiograph). Bone marrow cavity is filled with unresorbed bone in *NFATc1*$^{-/-}$ FLC chimera. (C) Histologic examination of tibia (top: toluidine blue staining; middle: tartrate-resistant acid phosphatase [TRAP] staining for detection of osteoclasts and lumbar vertebra; bottom: toluidine blue staining). No osteoclasts are observed in *NFATc1*$^{-/-}$ FLC chimera. (D) Histomorphometric evaluation of osteoclasts in *NFATc1*$^{+/-}$ and *NFATc1*$^{-/-}$ FLC chimera. (E) Reconstitution of the hematopoietic system of chimeric mice by the donor cells. PCR primers specific for joint region between the *NFATc1* locus and the neomycin-resistant gene (*NFATc1 neo*) and for wild-type (WT) *NFATc1* gene are used. The similar chimeric ratios were confirmed by quantitative PCR. (F) Complete blockade of in vitro osteoclastogenesis in osteoclast precursor cells from *NFATc1*$^{-/-}$ FLC chimera. Splenocyte-derived osteoclast precursor cells were cultured in RANKL (50 ng ml^{-1}) and M-CSF (10 ng ml^{-1}). We counted multinucleated (>3 nuclei) cells (MNCs) positive for TRAP staining. (G) Radiographic analysis of neonates generated by *Fos*$^{-/-}$ blastocyst complementation. Note the difference in radio-opacity at the femur (arrowheads). Right panels show the magnified view of the femur of neonates and tooth eruption of 6-wk-old mice. All of the *Fos*$^{-/-}$/*NFATc1*$^{-/-}$ chimeric mice exhibited osteopetrosis, but osteoclastogenesis is restored in *Fos*$^{-/-}$/*NFATc1*$^{+/+}$ chimeric mice when ES cells are transmitted to the hematopoietic system of recipient mice. **P < 0.001 versus control.

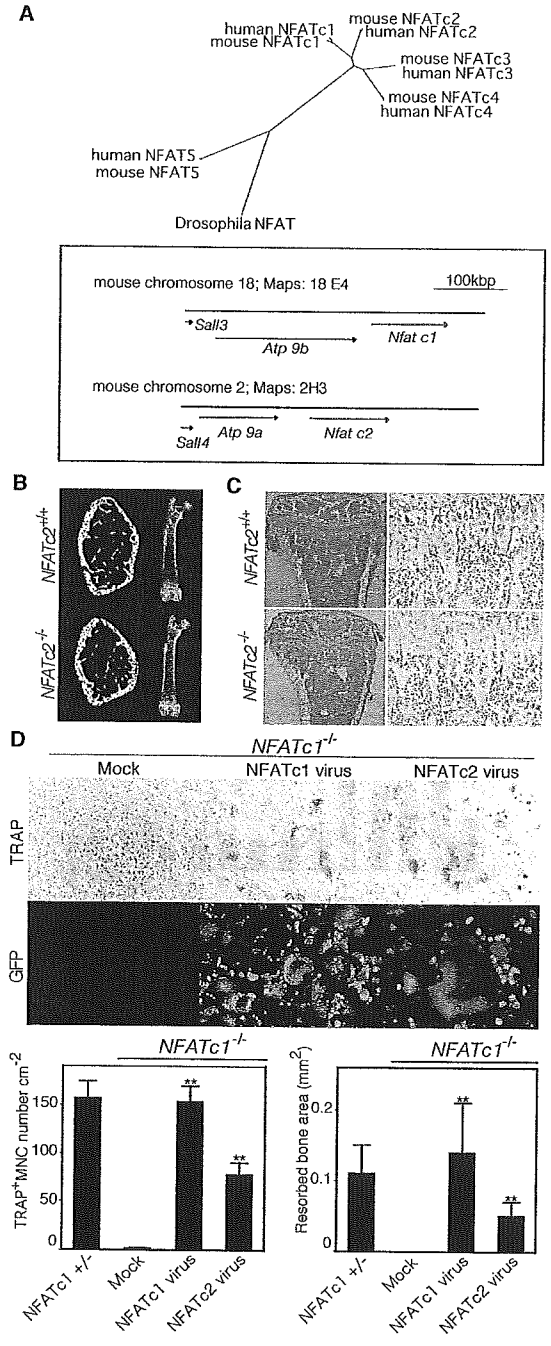

Figure 2. In vitro compensation of *NFATc1* deficiency by forced expression of NFATc2. (A) Phylogenetic tree analysis for the DNA binding (Rel homology) region of NFAT family proteins (top). A wide-range genomic view of *NFATc1* and *NFATc2* genes suggests that these genes were generated by chromosomal gene duplication (bottom). (B) Loss-of-function analyses of *NFATc2* in osteoclast differentiation. Microradiographic analysis of femur derived from *NFATc2*$^{-/-}$ mice at 5 wk of age (see Fig. 1 B). (C) Histologic examination of tibia from *NFATc2*$^{-/-}$ mice (left: toluidine blue staining; right: tartrate-resistant acid phosphatase staining [TRAP]). (D) Recovery of osteoclastogenesis in *NFATc1*$^{-/-}$ FLCs by retrovirus-mediated expression of NFATc1 or NFATc2. Forced expression of NFATc2 as well as that of NFATc1 induces formation of osteoclasts with pit-forming activity on dentin slices (RANKL, 50 ng ml^{-1}). Infection efficiency was monitored by GFP, which is expressed bicistronically. **$P < 0.001$ versus mock.

rated and bone marrow cavities are observed when *NFATc1*$^{+/-}$ FLCs are transferred to *Fos*$^{-/-}$ mice (Fig. 1, A and B). Tooth eruption, which is not seen in *Fos*$^{-/-}$ mice (13), is observed in these mice (unpublished data). In contrast, when *NFATc1*$^{-/-}$ FLCs are transferred to *Fos*$^{-/-}$ mice, they exhibit severe osteopetrosis and bone marrow cavities remain occupied with unresorbed bone (Fig. 1, A and B). Histologic analyses show that osteoclast number and parameters of bone resorption are normalized only when *NFATc1*$^{+/-}$ cells are transferred (Fig. 1, C and D). Repopulation of hematopoietic cells was confirmed by PCR in splenic lymphocytes and monocyte/macrophage precursor cells (Fig. 1 E). Consistently, osteoclast precursor cells that were derived from the *NFATc1*$^{-/-}$ FLC chimera could not generate osteoclasts in culture (Fig. 1 F). These results indicate that *NFATc1* is indispensable for osteoclast formation in vivo, and that FLC transfer to osteoclast-deficient mice is a beneficial tool for in vivo analysis of the osteoclast lineage.

Fos$^{-/-}$ blastocyst complementation

Rag-2–deficient blastocyst complementation is an alternative method for analyzing the lymphocyte-specific functions of gene, loss of which results in embryonic lethality (14). To provide additional genetic evidence for the essential role of *NFATc1* in osteoclastogenesis, we applied this method to an analysis of the osteoclast lineage using *Fos*$^{-/-}$ blastocysts (referred to as *Fos*-deficient blastocyst complementation). We analyzed chimeric neonates that were generated by injection of wild-type or *NFATc1*$^{-/-}$ embryonic stem (ES) cells into *Fos*$^{-/-}$ blastocysts. The chimeric mice that result from injection of normal ES cells into *Fos*$^{-/-}$ blastocysts (*Fos*$^{-/-}$/*NFATc1*$^{+/+}$ chimera) should develop mature osteoclasts, which are derived from the injected ES cells. In fact, all of the chimeric mice recovered from osteopetrosis, and tooth eruption was observed when the injected ES cells were transmitted into the hematopoietic lineage (Fig. 1 G). In contrast, chimeric mice that result from injection of *NFATc1*$^{-/-}$ ES cells into *Fos*$^{-/-}$ blastocysts (*Fos*$^{-/-}$/*NFATc1*$^{-/-}$ chimera) remain severely osteopetrotic, and have a defect in tooth eruption that is due to a lack of osteoclasts (Fig. 1 G and not depicted). Taken together with the results of FLC transfer, these observations provide clear evidence that *NFATc1* is essential for osteoclast differentiation in vivo.

NFATc2 is dispensable for osteoclastogenesis in vivo and in vitro

NFATc2 is another NFAT protein that is expressed at a low level in osteoclast precursor cells (5, 7). In addition to the similarity of the DNA binding (Rel homology) domain, the genomic view of the *NFATc1* and *NFATc2* loci suggest that NFATc2 is the evolutionally closest relative of NFATc1 among the NFAT proteins (1, 2, 15, 16) (Fig. 2 A). In addi-

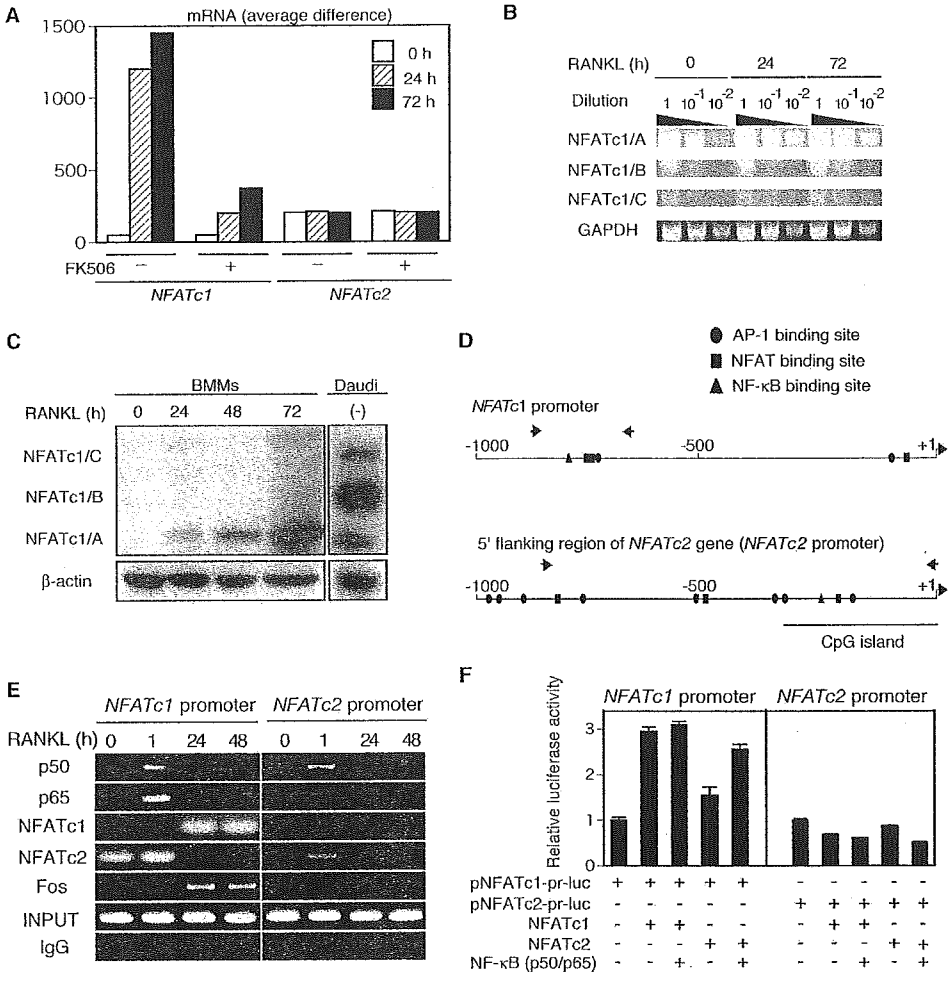

Figure 3. Autoamplification of *NFATc1* during osteoclastogenesis. (A) GeneChip analysis of mRNA expression of *NFATc1* and *NFATc2* in RANKL-stimulated BMMs. Strong induction of *NFATc1* by RANKL is inhibited by FK506 (2.5 μg ml^{-1}), which inhibits NFAT activity. NFATc2 expression is constitutive and is not affected by FK506. (B) Semiquantitative RT-PCR analysis of the mRNA of NFATc1 isoforms in BMMs. NFATc1/A is induced ~10-fold by RANKL. (C) Immunoblot analysis of NFATc1 isoforms during RANKL-induced osteoclastogenesis in BMMs. A Daudi lymphoma cell line is shown as a positive control for all three isoforms (A, B, and C) of NFATc1 (22). (D) A schematic illustration of putative transcription factor binding sites in the 5′ flanking region of the *NFATc1* (20) and *NFATc2* genes. Binding sites in the 5′ flanking region of the *NFATc2* gene were determined by the TRANSFAC retrieval program. Arrows indicate primers for ChIP experiments. (E) ChIP assay of *NFATc1* and *NFATc2* promoters in RANKL-stimulated BMMs. (F) Luciferase assay of *NFATc1* and *NFATc2* promoters in HEK293T cells.

tion, overexpression of NFATc2 facilitates the differentiation of osteoclasts (7) (Fig. S1, available at http://www.jem.org/cgi/content/full/jem.20051150/DC1). These results prompted us to investigate osteoclast differentiation in *NFATc2*-deficient (*NFATc2*$^{-/-}$) mice (17). Although NFATc2 is involved in the regulation of chondrocytes at advanced age, bone development of *NFATc2*$^{-/-}$ mice has never been well defined (18). Skeletal development occurs normally, and we observed no increase in bone mass in *NFATc2*$^{-/-}$ mice as shown in Fig. 2 B [see also reference 19]. We found no abnormality in the number of osteoclasts, or in the parameters of osteoclastic bone resorption (Fig. 2 C and Fig. S2, available at http://www.jem.org/cgi/content/full/jem.20051150/DC1) in *NFATc2*$^{-/-}$ mice. Consistently, *NFATc2*$^{-/-}$ BMMs that are stimulated by RANKL normally differentiate into osteoclasts with bone-resorbing activity (Fig. S3, available at http://www.jem.org/cgi/content/full/jem.20051150/DC1 and not depicted). In addition, RANKL induction of NFATc1 in *NFATc2*$^{-/-}$ cells is comparable to that in *NFATc2*$^{+/+}$ cells (Fig. S3). Thus, *NFATc2* is dispensable for RANKL-induced NFATc1 expression and osteoclastogenesis.

Osteoclast differentiation of *NFATc1*-deficient cells is rescued by forced expression of NFATc2

Because NFATc1 and NFATc2 have a similar ability to activate gene expression in T cells (1–3), it has been unexpected that *NFATc1* plays a nonredundant role in the skeletal system. *NFATc1*$^{+/-}$ cells differentiate into osteoclasts with bone-